2014

Potential Impacts of Changes in Climate on Water Quality in New York City's Ashokan

Nicholas Rossi

Potential Impacts of Changes in Climate on Water Quality in New York City's Ashokan Reservoir

A Masters Project Presented

by

Nicholas Rossi

Approved as to style and content by:

_____

Richard Palmer, Chairperson

_____

Casey Brown, Member

_____

Sanjay Arwade

Civil and Environmental Engineering Department

Abstract

This thesis investigates an approach for determining water resources vulnerability caused by climate change and applies it to a case-study for the New York City Water Supply System (NYCWSS).The results provide potential responses of the system to changes in climate and guidance that can inform short and long-term planning decisions. This research models the hydrology and operations of the NYCWSS and includes a statistical model of turbidity concentration in the Ashokan Reservoir. Using a stochastic weather generator, incremental changes are made to precipitation and temperature and used to drive the coupled hydrology-simulation model. The results are aggregated and examined to show the sensitivity of the system, and in particular Ashokan Reservoir turbidity, to changes in climate. The results are briefly compared with the latest GCM data to provide insight into expected changes in turbidity over the next half-century.

Table of Contents

List of Figures

List of Tables

List of Equations

1. INTRODUCTION

1.1. Planning in Water Resources

This thesis investigates an approach for determining water resources vulnerability caused by climate change and applies it to a case-study for the New York City Water Supply System (NYCWSS). The results provide potential responses of the system to changes in climate and guidance that can inform short and long-term planning decisions. Well-informed water resources planning is required to design, build, and operate the infrastructure related to the regulation of water. Such infrastructure includes dams, reservoirs, levees, flood-plains, supply systems, and spillways. Traditionally, these projects are planned using a cost-benefit approach: rather than protect against the entire realm of possible extreme events, designs are selected to minimize the combination of risks and costs of hazards while maximizing benefits (Stakhiv, 2011). Events used to plan (design events) are chosen based on the product of their probability of occurring and the potential damage from their occurrence. This planning strategy is predicated on the ability to accurately project the risks and potential costs that these ─hazardsø may cause. Until recently, these risks have been categorized by the assumed stationarity of the hydrologic cycle. Stationarity is the concept that natural systems fluctuate within a fixed envelope of variability; this implies that the probability density function of a variable can be estimated from an instrument record (Milly et al., 2008), or more simply, that an event of a certain magnitude has a direct probability associated with it that can be derived from the historic record.

Recently, an ideological shift in the field of water resources has called for an alternative planning and management strategy that is not predicated on stationarity (Milly

et al., 2008). This shift has occurred due to the growing body of literature documenting the changes in the Earth's climate. The National Climate Assessment (NCA; USGCRP, 2013) has reported that recent observations of the Northeast U.S. show warming and an increase in heavy precipitation events. These extreme events, as well as other changes, have been occurring with greater frequency in many parts of the world (Intergovernmental Panel on Climate Change, 2012).

This paper demonstrates a method that can be used to estimate the impacts of climate change in a water resources management setting. The risk of the associated changes in climate can be estimated by aggregating the results of a multitude of climate projections and both the risks and costs can be used in cost-benefit planning (Brown et al., 2011). This systemic cataloging of threats to the system, their costs, and their likelihoods (as well as system assets and capabilities) is a vulnerability analysis and it acts as the first of the four common stages in water resources planning (WUCA, 2010). Computer models are used to conduct vulnerability analyses to illustrate the impacts of various potential scenarios. Computer models can simulate the behavior of reservoir systems and associated hydrology to allow planners to test for sensitivities. The information in the vulnerability analysis can be used to guide planning, allowing emphasis to be placed on portions of the system that are susceptible to failure. Historically, the water industry has used the stationarity assumption when performing vulnerability analyses of water systems, using the historic record to drive the simulation models. Recognizing the recent changes in hydrologic stationarity, new approaches are necessary to incorporate climate change scenarios into water resources vulnerability analyses (WUCA, 2010). The approach described in this paper draws heavily on the

current water resources and climate change literature to incorporate the new criteria for a water resources vulnerability analyses.

1.2. Planning Under Climate Change

There are two common planning approaches used to incorporate climate change into vulnerability analyses. For the purposes of this discussion, they will be described simply as a top-down approach and a bottom-up approach (Dessai and Hulme, 2004). The top-down approach is scenario-driven with the basic premise being to plan for specific events, or a range of events, guided either by climate-science data or by scenarios that are generated to explore a range of potential futures. The bottom-up approach focuses on the system characteristics under investigation with the goal of gathering specific information on the water resources system of interest.

In the context of climate change, top-down vulnerability analyses generally make use of General Circulation Models (GCMs, also referred to as Global Climate Models) for projections to drive the water resources model. GCMøs are mathematical models that simulate the earth-atmosphere system and can use a number of greenhouse gas emission scenarios supplied from the IPCC as inputs (Kisparsky et al., 2012). Outputs from these models include projections of temperature, precipitation, and other climate-related variables; the output from these models inform the vulnerability analyses by projecting the hazards the system will face under climate change and the resulting costs of the hazards.

GCM models are selected on a study-by-study basis, often based upon their ability to replicate past, observed conditions. It is often necessary to bias-correct these models during the verification process to more accurately reproduce historic climate. To

achieve the resolution necessary for watershed-scale simulations, GCM outputs are "downscaled" using a variety of emerging techniques that are tailored to the specific study (Wilby et al., 2004). The climate models are then driven with a selection of emission scenarios to produce a range of output variables. Water resource planning studies will typically incorporate more than one GCM by creating model ensembles.

Results from the GCM simulations are used to select input variables for local hydrology models, such as temperature, precipitation, wind speed, radiation, and humidity. The hydrology model simulates the physics of the basin to project time-series values of the variables that will drive the system simulation models used for planning studies, such as snowmelt and streamflow (Wiley and Palmer 2008; Christensen et al., 2004). Studies directly incorporating GCM outputs are typically applying the top down approach, as the planning is tailored to the scenarios projected by the GCM's.

The use of GCM projections as inputs to water resources models to categorize risks has been questioned because of the uncertainty associated with the projections. Uncertainty in water resources modeling is inescapable and arises from a variety of sources, including a lack of understanding of the physical system (short historical record, poor characterization of hydrology), the social system (changing water demands, changing social priorities), or the economic system (changing prices). Uncertainty is also inescapable with GCM's because the resolutions of the models is much coarser than needed for watershed basins, in fact, their original intent was to project the effects of various greenhouse gas emission scenarios on the Earth's atmosphere (Kundzewicz, 2010). The limitations of GCM to replicate past climate and the uncertainties if using them to forecast projections are well documented but seem to be irreducible with the

current versions of the models (WUCA, 2009). To be useful in hydrology models, GCM results must be downscaled regionally and bias corrected and this also introduced new sources of uncertainty. (Kundzewicz, 2010). Projections also muddle the ﹣riskø term used in a cost-benefit approach to planning, as there is no exact uncertainty range, or probability estimate, to the individual projections.

Bottom up vulnerability analyses are focused on the responses of the system to various scenarios and have been used recently by planners to understand the risks to water systems (Jones, 2001; Lempert et al., 2004). As early as 1962, engineers began taking advantage of the rising computational power available by creating unlimited records of synthetic input data that conformed to the observed characteristics of the local historic data in order to study the responses of their system models (Thomas and Fiering, 1962). This method has been more recently adapted to suit climate change vulnerability analyses by using input data that resembles climate change projections rather than historic weather.

The methodology used in this thesis closely resembles the bottom-up climate change vulnerability analyses though it draws more specifically from the decision-scaling method recently introduced to water resources literature (Brown et al., 2011). Decision-scaling combines a number of bottom-up analyses to determine the stress on a system caused by changes in climate. The desired basin climate statistics are incrementally varied when creating time-series of synthetic weather to produce different scenarios (Brown and Wilby, 2012). The resulting system performance associated with the different scenarios are analyzed and related to the climate statistics that produced the scenario. Different thresholds of acceptable values of system variables can be determined

with the help of the system stakeholders and acceptable levels of change that produce results up-to but not including the threshold values can be determined. Decision-scaling then utilizes available climate information to determine the risk, or probability, that the threshold values will be exceeded. (Brown et al., 2012; Moody and Brown, 2012)

  With very large systems, such as with the New York City Water Supply System, bottom-up and decision-scaling style vulnerability analyses can require extensive amounts of time and resources because of the large number of scenarios. This study demonstrates the effectiveness of a bottom-up style vulnerability analysis using a screening tool simulation model to facilitate rapid turnover and analysis of a wide-range of climate change scenarios. The screening tool consists of a simplified water resources simulation model created to simulate operations accurately and quickly.

2. PROBLEM BACKGROUND

2.1. New York City Water Supply System (NYCWSS)

Today, the New York City Water Supply System (NYCWSS) delivers approximately 1.04 billion gallons of water per day to the more than nine million consumers in New York City and the four surrounding counties that border on the City and the supply system. Water demands peaked in 1979 at about 1.5 billion gallons per day and have been near or below 1.1 billion gallons per day since 2003. The major supply components of the system have been in place since 1964. The New York City Department of Environmental Protection (NYCDEP) is responsible for the operation and maintenance of the NYCWSS as well as investment planning. The Bureau of Water Supply, within the NYCDEP, is responsible for managing, operating, and protecting the water supply system and watersheds. The NYCWSS places an emphasis on source water protection programs resulting in repeated Filtration Avoidance Determinations (FADs) from the United States Environmental Protection Agency (EPA), with the most recent 10-year FAD issued in July 2007. The FAD maintains New York City's status as one of only five large cities in the country with a surface drinking water supply of such high quality that filtration is not required. These five cities are: Seattle, WA; Portland, OR; San Francisco, CA; Boston, MA; and New York, NY (Alcott et al., 2013). As part of the agreement, New York City continues to enhance existing watershed protection programs while developing new efforts such as land acquisition, land management, and partnerships with local environmental and non-profit organizations (NYCDEP, 2012).

The system stores water in three upstate reservoir systems that include 19 reservoirs, three controlled lakes and a total storage capacity of approximately 580 billion

gallons. The watersheds providing this water are approximately 2,000 square miles. Three separate water supply subsystems compose the NYCWSS: the Croton system is located just North of NYC in Westchester County and contains 12 reservoir basins, the Catskill/Delaware system, referred to together as the West-of-Hudson (WOH) system, consist of six reservoirs located as far as 125 miles North and West of NYC, and a groundwater system in the Queens borough of NYC (Figure 1). The separate water collection systems were designed and built with various interconnections to increase flexibility by permitting exchange of water from one to another. This feature mitigates localized droughts and takes advantage of excess water in any of the systems. (NYCDEP, 2014a).

Figure 1. Schematic of the NYCWSS (NYCDEP, 2007)

The Croton system is used as a transfer station for WOH water heading towards

the city though in times of low supply the Croton system is drawn down to meet demand.

Use of the groundwater supply is limited to emergencies. In 2012, 100% of the drinking water was supplied by the WOH system (NYCDEP, 2012). The WOH supply can be divided into two systems: the Delaware system and the Catskill system; on average, the Delaware system provides 60 percent of the city's daily water needs while the Catskill system provides the other 40 percent. The Delaware system contains three reservoirs that operate in parallel, Cannonsville (95.7 billion gallon capacity), Neversink (34.9 billion gallons capacity), and Pepacton (140.2 billion gallon capacity), feeding into a fourth reservoir, Rondout (49.6 billion gallon capacity). The Catskill system contains two reservoirs that operate in series, with the Schoharie Reservoir (17.6 billion gallon capacity) feeding the Ashokan Reservoir (122.9 billion gallon capacity). Water from Rondout reservoir travels via the Delaware Aqueduct through the Croton system and the Kensico Reservoir (30 billion gallon capacity) on the edge of the Croton system before entering the NYC distribution system. Likewise, water from the Ashokan Reservoir travels directly to the Kensico Reservoir via the Catskill Aqueduct before entering the NYC distribution system.

The Delaware system is located in the Western portion of the Catskill Mountain Range in the headwaters of the Delaware River. The Delaware River is regulated by the Delaware River Basin Commission (DRBC), a regional body created in a 1961 agreement between the federal government and the four states which share the Delaware River and its watersheds: Delaware, New Jersey, Pennsylvania, and New York. This body was created 7 years after a U.S. Supreme Court decree in 1954 in the case of New Jersey v. New York which established minimum releases from the reservoirs downstream to the Delaware River ensuring equitable allocation of the region's resources. The DRBC

is currently responsible for ensuring all parties, including the NYCDEP, are abiding to the code, regulations, and rules of practice established by the Supreme Court decision.

The New York City Bureau of Water Supply's (NYCBWS) primary mission is to ensure the delivery of a sufficient quantity of high quality drinking water. As noted previously, the quantity of water provided by NYCBWS has steadily decreased for the past four decades with current demand nearly 40% below 1980s levels despite a 15% growth in population. The most recent safe yield estimates for the system are between 1,225 and 1,370 MGD, with the higher range of values including infrastructure improvements that are not yet completed. The safe yield of this system is defined by the drought of the 1960s. Safe yield projections exceed projected water demands by 11% (NYCDEP, 2011), signifying that the NYCWSS faces very little risk of being unable to deliver a sufficient quantity of water, even in worst-case scenarios. Maintaining the high quality of the drinking water is the highest priority for the NYCBWS.

One component of the NYCWSS that has required special attention is the Ashokan Reservoir, which has periodic turbidity events, a water-quality parameter regulated under the Safe Drinking Water Act (1974). This reservoir has been closely monitored by the NYCDEP to ensure that drinking water meets all regulatory requirements and in 2013 the NYCDEP agreed to an updated constraint order with the NYC Department of Environmental Conservation (NYCDEC) to further regulate and monitor the water quality in the Ashokan Reservoir

2.2. Turbidity in the Ashokan Reservoir

The Ashokan Reservoir is located in Ulster County, about 13 miles west of Kingston and 73 miles north of New York City. Located on Esopus Creek, the dam and

reservoir consists of two basins separated by a concrete dividing weir and roadway. The facility was placed into service in 1915 and has a capacity of 122.9 billion gallons. It has a watershed drainage basin of 255 miles that includes parts of 11 towns (NYCDEP, 2014b). Average flows into the reservoir are approximately 350 MGD.

The Ashokan is one of two reservoirs in the Catskill Water Supply System. The other is the Schoharie, located 27 miles to the north. Schoharie's releases flows into the Ashokan via the Shandaken Tunnel and the Esopus Creek. Including transfers from the Schoharie Reservoir, the Ashokan supplies about 40% of New York City's daily drinking water in non-drought periods. Water enters the Ashokan's West Basin and, after a settling period, is typically transferred to the East Basin by a gate in the dividing weir. During special circumstances, such as a large event, water may spill over the weir into the East Basin or be released from the West Basin to the downstream portion of Esopus Creek. From the East Basin, water is transported southeast under the Hudson River via the 92-mile Catskill Aqueduct, which has a maximum depth of 1,114 feet. It ordinarily enters the Kensico Reservoir in Westchester for further settling, where it mixes with Delaware system water and then travels south in two aqueducts before entering New York City's water supply distribution. (NYCDEP, 2014b)

The foremost operational challenge in managing the Ashokan Reservoir is periodic turbidity events in the West Basin. The source of the turbidity is clay mineral particles that are transported from the Esopus Creek watershed during storms. Extensive stream channel erosion of glacial clay deposits has been identified as the main cause of high levels of turbidity in many of the tributaries draining the Catskill watersheds (Nagle et al., 2007). The vast majority of eroded sediments in all streams are transported during

high flow events (Wolman and Miller, 1960). Increases in reservoir turbidity impacts water quality and has the potential to affect the NYCWSS operations when water in Ashokanøs West Basin is too turbid to be transferred to the East Basin (Effler et al., 1998; Gelda et al., 2009). In this case, the East Basin is drafted lower than desired by the NYCDEP, leaving the system vulnerable to subsequent large rainfall or drought events.

2.3. Climate Change and the NYCWSS

The NYCDEP, NYCBWS, the New York State Department of Environmental Conservation, the NYC Department of City Planning, and other New York City and New York State agencies have been leaders in defining the impacts of climate change on New York City and in exploring a range of management alternatives (NYCDEP, 2008). One example of this is the formation of the Second New York City Panel on Climate Change (NPCC2). This group includes leading climate and social scientists and risk management experts charged with advising the Mayor of New York City on issues related to climate change and adaptation as well providing up-to-date scientific information and analyses on climate risks. The latest report from NPCC2, õClimate Risk Information 2013 ó Observations, Climate Change Projections, and Mapsö (New York City Panel on Climate Change, 2013) presents observed data from the past century, results of GCM simulations from the Coupled Model Intercomparison Project Phase 5 (CMIP5), and data developed for the upcoming IPCC Fifth Assessment Report (AR5). The observed and projected climates for New York City are summarized in a regional and global context, with an emphasis on observed trends over large spatial scales (New York City Panel on Climate Change, 2013).

The report indicates the following: Temperature and precipitation trends indicate overall increases from 1900 to 2011 in New York City but with inter-annual and decadal variations; temperature has increased by 4.4 °F and precipitation has increased by 7.7 percent. There has also been evidence of increasing variability in year-to-year precipitation in NYC when comparing the first half of the 20th century to the second half. The temperature trends are broadly similar to the trends for the entire Northeastern United States; the precipitation trends in the Northeast are similar but cannot necessarily be distinguished from natural variability (New York City Panel on Climate Change, 2013).

Extreme events are climate occurrences that are especially intense and can have significant impacts on New York City. These can include heavy rainfall, heat waves, and coastal floods. There is rarely statistical significance in the evidence at local scales to unveil trends in extreme events because of high natural variability and limited record length (Horton et al., 2011). At regional and global scales there can be statistically significant trends; changes in extreme events at these spatial scales have been attributed to human influences on the global climate (IPCC, 2012). There has been a slight trend towards an increase in extreme precipitation events in New York City since 1900, though it cannot be distinguished statistically from random variability (New York City Panel on Climate Change, 2013). Over the larger Northeast U.S. region, there has been an approximately 70 percent increase in intense precipitation events (defined as the heaviest 1 percent of all daily events) over the period from 1958 to 2011 (USGCRP, 2013).

The NPCC2 report provides climate projections for the 2020s and 2050s (Table 1). As in all climate forecasts, the report notes that the precipitation projections are

considered less certain than the temperature projections with some climate models suggesting an increase in precipitation and other suggesting a decrease (New York City Panel on Climate Change, 2013). The report also notes that there are several reasons why future climate changes may not conform to these forecasts, noting potential changes in greenhouse gas emissions, potential changes to the climate's sensitivity to greenhouse gases, and other climate changes outside model-based estimates. It is also important to recognize that although the projections show relatively small percentage increases in annual precipitation, larger percentage increases are expected in the frequency, intensity, and duration of extreme precipitation at daily timescales (New York City Panel on Climate Change, 2013).

Table 1. NYC Climate Projections

Air Temperature Baseline (1971 - 2000) 54 °F	Low-estimate (10th percentile)	Middle range (25th to 75th percentile)	High-estimate (90th percentile)
2020s	+1.5 °F	+2.0 °F to 3.0 °F	+3.0 °F
2050s	+3.0 °F	+4.0 °F to 5.5 °F	+6.5 °F
Precipitation Baseline (1971 - 2000) 50.1 inches	**Low-estimate (10th percentile)**	**Middle range (25th to 75th percentile)**	**High-estimate (90th percentile)**
2020s	0 percent	0 to +10 percent	+10 percent
2050s	0 percent	+5 to +10 percent	+15 percent

Recent studies of the NYCWSS using GCM projections conclude that the water supply system will most likely continue to be highly robust, indicating a low probability that the system will experience failure due to a water shortage and, that if low storage occurs, it will likely return to more normal conditions quickly (Matonse et al., 2012). This positive outlook for the NYCWSS supply variables is due in part to a rise in monthly inflows for almost all months with the greatest changes during winter and early spring due to a combined effect of more rainfall and snowmelt associated with higher

temperatures (Matonse et al., 2011). The Matonse et al (2012) study concluded that under the climate change projections the reservoirs will fill earlier with inflows more evenly distributed during winter and early spring, shifting the peak spring runoff earlier into the winter. The study also projected a decrease in the average number of days that both the Catskill and Delaware reservoir systems would be under drought emergency, warning, or watch conditions. Equally important, water demands for the region have decreased dramatically making a water shortage less likely now and in the next several decades.

2.3.1. Climate Change and Turbidity

Because high flows in the streams that supply water can result in turbidity events, the overall number of turbidity events is expected to increase as monthly inflows to the reservoirs increase due to higher average values of monthly precipitation. In addition, the timing of snowpack runoff is expected to change due to increase in temperature. The potential for an increase in extreme precipitation events with climate change also presents a potential for increased erosion and subsequent turbidity events. Studies simulating climate change scenarios have resulted in annual Ashokan West turbidity increases of 3% and 5% for the 2050s and 2090s, respectively (Samal et al., 2013). Additionally, the study found that the average winter reservoir turbidity increased by 11% and 17% for the 2050s and 2090s, respectively, while the turbidity from April to May decreased, though peak average turbidity still occurs in April. This projected change in the turbidity seasonality is attributed to the shifting of the peak spring runoff earlier into the winter, resulting in higher winter streamflows and lower spring streamflows. The Samal et al. (2013) study simulated climate change using three GCMs and three future emission scenarios.

2.4. Project Goals and Objectives

The goal of this research is to identify climate-related vulnerabilities of the NYCWSS to inform future decision-making and operations. Because the NYCWSS will likely maintain high resilience, high annual reliability, and relatively low water-supply vulnerability in the future, the research focuses on the system vulnerability to turbidity events, as the NYCDEP has identified this as a topic of great interest.

This project utilizes an analysis approach that assesses the sensitivities of the system to incremental changes in climate by testing their impacts in a simulation model that includes both water balances, turbidity modeling, and detailed systems operations. A synthetic weather generator is used to create time-series with adjustments to the annual statistics of precipitation and temperature. The nature and range of scenarios can be determined through stakeholder discussion and are not necessarily confined to being likely, or even plausible, but instead to allow the researchers to determine sources of vulnerability in the system (Brown and Wilby, 2012).

Previous studies conducted by the NYCDEP and associated partners have led to the development of The Operational Analysis and Simulation of Integrated Systems (OASIS) model (HydroLogics Inc., 2007) and the Operations Support Tool (OST), both used by operators and managers to support NYCWSS operations and planning (NYCDEP, 2010). The NYC OASIS model has also been linked to a Qual-W2 water quality model (referred to as OASIS-W2) that is capable of estimating in-reservoir contaminant concentrations (Cole and Wells, 2002). Both the OASIS-W2 model and the OST are very sophisticated models, with relatively demanding computational requirements. Since a research goal is to explore a large number of future scenarios, the

computational requirements of using these models for the analysis appeared to preclude their use. To conduct this research, a õscreening-toolö model is needed that allows rapid evaluation of each scenario. Climate scenarios that expose vulnerabilities in the system can be identified, investigated further, and then examined in great detail in OASIS and in the OST. Further investigation identifies different weather and hydrologic regimes on various time-scales that are causing the system vulnerabilities as well as the projected likelihood of the scenario.

The general approach for this research is to generate, test, and interpret incrementally-changing climate scenarios and their impacts on the NYC water supply. The research objectives are as follows:

1) Generate synthetic time-series of precipitation and temperature that capture trends in the historic data but allow for adjustments to mean precipitation and mean temperature.

2) Test a wide-range of precipitation and temperature scenarios in a screening tool that accurately simulates the hydrology and operations of the NYCWSS.

3) Analyze these results and develop climate response functions for system variables of interest. Specifically this includes identifying the climate drivers of turbidity in the Ashokan Reservoir.

3. METHODOLOGY

3.1. Model Framework

The project utilizes three separate computer models to generate the desired results. The models used are: 1) a multivariate, multisite daily weather generation model, 2) a watershed hydrology model, and 3) a reservoir operations screening tool model. The modeling process proceeds logically from changes in climate, to impacts on hydrology and then to systems operations. The three models were loosely integrated using the statistical computing program R (R Core Team, 2012) to execute iterative, batch files as well as for the aggregation of model outputs and data analysis.

3.2. Weather Generator

A semi-parametric multivariate, multisite weather generator (Steinschneider and Brown, 2013) is used that employs an autoregressive model to simulate annual climate conditions and a Markov chain and k-nearest-neighbor (KNN) resampling method to simulate daily weather variables. The model allows for changes to be made to mean precipitation, mean temperature, and precipitation variance by a quantile mapping procedure to simulate a range of climate changes. The model operates in R.

Historic daily climate data consisting of precipitation and maximum and minimum temperatures were gathered for each of the seven watershed areas of the West-of-Hudson reservoir systems over the period of January 1, 1950 to December 31, 1999 from the gridded observed meteorological dataset produced by Maurer et al. (2002). The observed precipitation data exemplified typical properties of the Northeastern U.S., with relatively infrequent and less intense storms in the winter and bimodal peaks in the spring and fall. These data were used to calibrate the weather generation model

The model was used to replicate daily precipitation and maximum and minimum temperature from the observed time period. Average monthly maximum and minimum temperatures were calculated from the model results for 50 separate model-runs of 50 years each, presented in Figures 2 and 3 with the historic values represented by the red triangles. Figure 4 shows a similar plot for average monthly precipitation. The model accurately and precisely replicated the observed temperature and predicts precipitation within the 25th to 75th percentile range for eight of the twelve months. The weather generator introduces some statistical variability when creating time-series of precipitation so it is expected that the simulated precipitation would vary slightly from the observed record of precipitation. Percent cumulative errors (Thomann, 1982) between simulated and observed, calculated using the formula in Equation 1, were low for all three variables, with the highest being 2% for precipitation over the 50-year comparison period, and maximum and minimum temperatures having values of 0.2 and 0.4 percent, respectively.
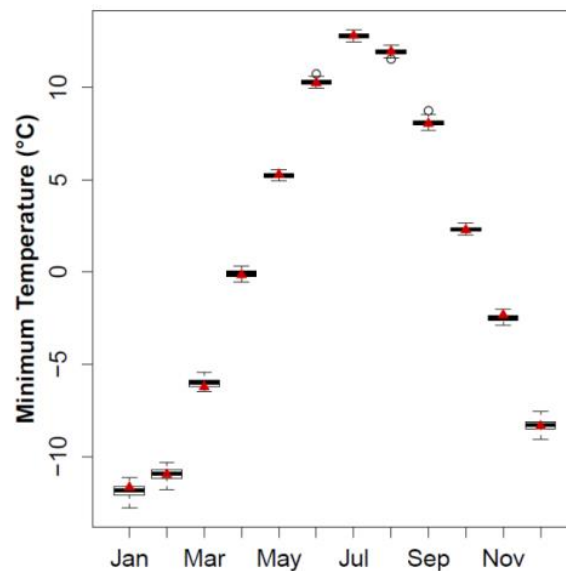
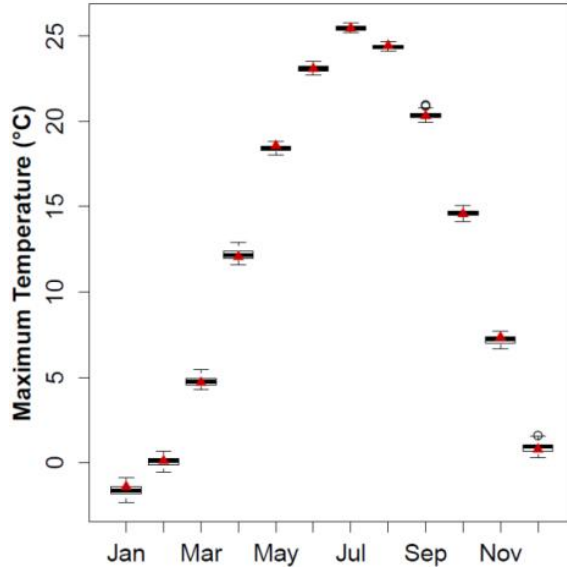**Figure 2. Minimum Temperature, Modeled and Historic**

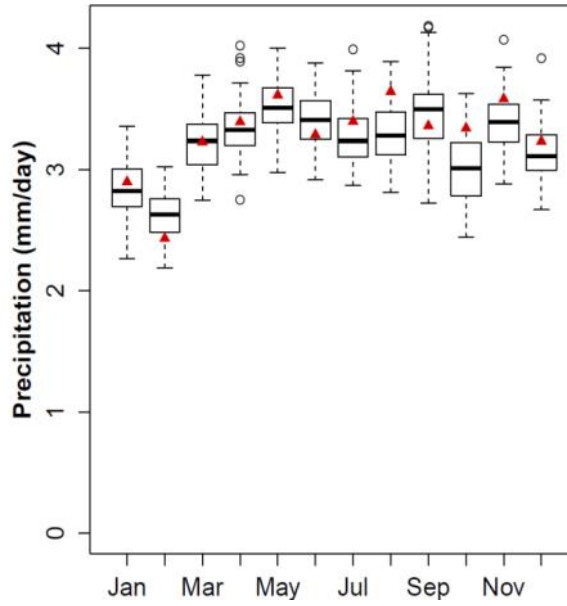**Figure 3. Maximum Temperature, Modeled and Historic**

Figure 4. Precipitation, Modeled and Historic

$$\% \qquad = \qquad \overline{\hspace{3cm}} \qquad\qquad (\,1\,)$$

3.3. GWLF Hydrology Model

Inflows to the each of the seven reservoirs are simulated on a daily time step using the Generalized Watershed Loading Functions-Variable Source Area (GWLF-VSA) watershed model (Haith and Shoemaker, 1987; Schneiderman et al., 2002; Schneiderman et al., 2007). The model was implemented in the computer simulation program Vensim DSS (Ventana Systems Inc., 2013). The GWLF-VSA is a lumped-parameter continuous simulation model that simulates daily stream flow and various water quality parameters on a watershed scale. Inputs to the model include air temperature, precipitation, incoming solar radiation and relative humidity. The outputs from the model used in this analysis are streamflow, snowpack depth, and potential evapotranspiration for each of the seven watershed basins. Historic observed incoming solar radiation and relative humidity are used as inputs to the hydrology model during the climate change analysis. Incoming solar radiation is based upon the reservoirsø position on the globe and is not expected to change under climate change scenarios. Relative humidity varies under the climate change scenarios, but the effects of relative humidity on the outputs of the model are small, as demonstrated by trial model runs with relative humidity values fixed at the 25th and 75th percentile values of their historic observed values for which the resulting time-series correlation values were above 0.999 for all reservoirs.

This hydrology model has been adopted by the NYCDEP Water Quality Modeling Group for the majority of their hydrologic analysis and has been extensively calibrated (Schneiderman et al., 2002; Schneiderman et al., 2007). Model results were verified for a selection of reservoirs and statistics. The verification statistics evaluated in

the calibration/verification process included the percent cumulative error, correlation (r), and the Nash-Sutcliffe Efficiency (Nash and Sutcliffe, 1970), presented in Equations 1, 2, and 3, respectively. These statistics were calculated for daily, monthly, annual, and annual maximum-daily flows in the Cannonsville, Neversink, and Schoharie watersheds between 1950 and 1975. The sites were chosen as a representative sample of the seven reservoirs modeled for this research, the observed flow values were obtained from the USGS archives. The GWLF reservoir model watershed area values were adjusted to represent the location of the gages as the outlets of the model. The statistics are available in Tables 2, 3, and 4.

$$= \frac{\Sigma(\quad * \quad) \ (\Sigma \quad)(\Sigma \quad)}{(\Sigma \quad) \ (\Sigma \quad) \ (\Sigma \quad) \ (\Sigma \quad)} \qquad (2)$$

$$= \quad - \frac{\Sigma(\qquad)}{\Sigma(\qquad \qquad)} \qquad (3)$$

Table 2. GWLF Correlation Coefficient Values

	Daily	Monthly	Annual	Annual Max Daily
Cannonsville	0.716	0.924	0.843	0.528
Neversink	0.797	0.941	0.929	0.67
Schoharie	0.786	0.905	0.88	0.744

Table 3. GWLF Cumulative Error Values (%)

	Daily	Monthly	Annual	Annual Max Daily
Cannonsville	3.98	4.12	5.63	18.26
Neversink	-4.2	-4.01	-4.58	-0.91
Schoharie	0.39	0.58	-0.54	10.28

Table 4. GWLF Nash-Sutcliffe Efficiency Values

	Daily	Monthly	Annual	Annual Max Daily
Cannonsville	0.379	0.838	0.416	-0.409
Neversink	0.622	0.874	0.822	0.387
Schoharie	0.555	0.818	0.754	0.241

The model is most effective on a monthly time-scale, but still exhibits strong correlation and low percentage cumulative error on daily time steps. Year-to-year, the model shows strong correlation between observed and simulated flows, with relatively low cumulative error. The Nash-Sutcliffe values for all time periods indicate that the model is a good fit and outperforms the observed means as a predictor of flows. For predicting the annual maximum-daily flow, the model performs relatively well considering the difficulty of capturing a single event in the course of a year, with the model proving to be a better predictor than the observed mean in two of the three cases and correlation values slightly above the ˉweakøcategory for all three watersheds.

3.4. STATS Screening Tool

The Screening Tool for the Assessment of Turbidity and Supply (STATS) was created to complete the proposed analysis of system sensitivity to climate changes. Similar to the GWLF model, STATS was constructed using Vensim software (Ventana Systems Inc., 2013). STATS is a mass balance model of the NYCWSS, assigning various amounts of water through the system loosely based upon a variation of the õSpace Ruleö known as the õNew York City Ruleö (Guzman and Lund, 1999). This rule defines releases from reservoirs based upon the probability of refill by June 1 to minimize the probability of spills and thus the minimization of expected shortages. The screening tool also incorporates all of the Federal and State regulations and agreements necessary to

accurately and precisely simulate the actual operations of the system. The full list of regulations used in STATS is available in APPENDIX A.

A critical component of the STATS tool is simulation of turbidity loading into the Ashokan West Reservoir as well as the total concentration of turbidity within the reservoir. STATS utilizes a multiple regression model derived from Mukundan et al. (2013) to predict mean daily turbidity flowing into the reservoir:

$$= . \quad (\quad) - . \quad + . \quad - . \tag{4}$$

Where: MDT = Mean Daily Turbidity (NTU)
$\quad\quad\quad$ Q_D = Stream Discharge (MGD)
$\quad\quad\quad$ SEASON = 1 for November thru April, otherwise 0
$\quad\quad\quad$ ADD = Antecedent Dry Days

The reservoir is assumed to be a completely-mixed reactor to predict a 0-order turbidity concentration within the reservoir. The size distribution of the sediment flowing into the reservoir is predicted based upon the flow into the reservoir. If flow is above 913 MGD, then the incoming sediment consists of 10 percent large, 45 percent medium, and 45 percent small particles; for flow below 913 MGD, the percentage distribution of large, medium, and small particles is 10, 65, and 25 percent, respectively (Gelda et al., 2009). STATS uses the size distributions of the suspended sediment to determine the settling rate of turbidity in both basins of Ashokan Reservoir, with larger particles settling more quickly than smaller particles (Gelda et al., 2009).

The rules governing the operations of STATS were manually calibrated to best match the observed annual, seasonal, and monthly storages. The accuracy of STATS in simulating storages, yields, and turbidity was verified using OASIS data to ensure accurate and precise results during the climate change analysis. STATS was verified

using OASIS-W2 data because the operations of the NYCWSS have changed drastically over the past 50 years and comparisons with historic storage and turbidity would not have reflected the ability of STATS to simulate current and future system operations and conditions. The OASIS-W2 model results were supplied by the NYCDEP Water Quality Modeling Group specifically to help in calibrating STATS; Table 6 displays the calculated correlations and Nash-Sutcliffe Efficiencies between the STATS model and the OASIS model for the 50-year period between January 1, 1950 and December 31, 1999.

Table 5. STATS Correlation and NSE Values

	Delaware Storage	Catskill Storage	Ashokan Storage	Ashokan West Turbidity	Ashokan East Turbidity
Correlation	0.964	0.946	0.936	0.690	0.688
NSE	0.877	0.759	0.805	0.302	0.268

STATS performs well when allocating storage in the NYCWSS, exhibiting high correlation and high Nash-Sutcliffe values for the entire 50-year period for both major subsystems (Delaware and Catskill) as well as for the Ashokan Reservoir (total of both East and West basins). STATS turbidity modeling exhibited medium correlation values in both the West and East basins; the Nash-Sutcliffe values were low in both basins but well above a 0-value, which would indicate the observed mean as a more accurate predictor than the model. Details on the calibration and verification of STATS are presented in DeChristofaro (2014).

3.5. Analysis

The weather generation model was used to create ensemble time-series of 40 weather scenarios. Each time-series contained 50 years of daily values of precipitation and temperature. Each scenario represented an incremental change in either precipitation, temperature, or both; mean temperature increased from 0 to 7 degrees Celsius at 1 degree increments and mean precipitation varied from 90% to 130% of the observed mean at 10% increments. For instance, the final of the 40 scenarios contained 50 years of daily precipitation and temperature with the annual average temperature fixed at 7 degrees Celsius above the mean and annual precipitation fixed at 130% of mean precipitation. This process was repeated 10 times to develop 10 separate õrunsö, each with the same 40 scenarios representing the equivalent annual statistics but producing different daily time-series because of the natural variability introduced by the model.

The weather time-series were used to drive the GWLF hydrology model, which outputted simulated streamflow values to be used as inflows for all seven of the NYCWSS reservoirs modeled in STATS. The STATS model simulated the operations of the system and the turbidity concentration of the Ashokan Reservoir.

To better understand the sensitivity of Ashokan Reservoir turbidity to changes in climate, a series of concentration values were selected that represented important limits for the operations of the NYCWSS. These threshold concentration values were selected with expertise input from the NYCDEP Water Quality Modeling Group and included two thresholds in Ashokan West, 10 and 25 NTU, and two thresholds in Ashokan East, 5 and 10 NTU. The Ashokan West threshold values were selected as general indicators of the total amount of turbidity caused by the changes in climate. The Ashokan East threshold

values were chosen because of their operational importance. When concentration exceeds 5 NTU, Catskill Aqueduct flow to the Kensico Reservoir is often reduced to an amount such that the product of concentration (NTU) and flow (MGD) is less than 3,000. When concentration rises above 10 NTU, the use of stop shutters within the aqueduct may be necessary to further reduce flow. These reductions in flow are necessary to keep turbidity concentrations low in the Kensico Reservoir and Croton Supply so as to not violate the terms of the Filtration Avoidance Determination from the EPA and they may put strain on other parts of the system. It is important to note that these operational decisions are not formal and actual operations are made based on the best available current information, such as quality and flow conditions and meteorological forecasts.

The number of times that the turbidity concentration exceeded the threshold was noted in the model for both reservoirs and all four threshold values. These binary time-series of turbidity threshold exceedances were summed over the 50-year simulation period by month and then averaged across the 10 runs for each of the 40 scenarios. The resulting data was used to draw conclusions between scenario characteristics (precip, temp) and the numbers of monthly turbidity threshold exceedances in that scenario.

4. RESULTS

4.1. Climate-altered Hydrology Results

Incremental changes in precipitation have relatively uniform effects on the inflows into the reservoir; as precipitation increases, inflows increase for all months (Figure 5). Incremental increases in precipitation causes the largest increases in inflows in the peak inflow month of April, while the increases in inflow are less in the summer and winter.

Incremental changes in temperature have dramatic effects on the seasonality of inflows into the Ashokan West Reservoir (Figure 6). Increasing temperature causes higher inflows from December to February, though there is a diminishing effect as the temperature increase approaches 4°C. Subsequently, flows from March until November are decreased, with the largest decreases in flow happening in April and May. These changes in the seasonality of inflows into the Ashokan West Reservoir are caused by the decrease of snowpack in the winter months, as precipitation falls as rain rather than snow in higher temperature scenarios. The resulting volume of inflow over the year is slightly reduced as temperature increases, due to an increase in evapotranspiration.
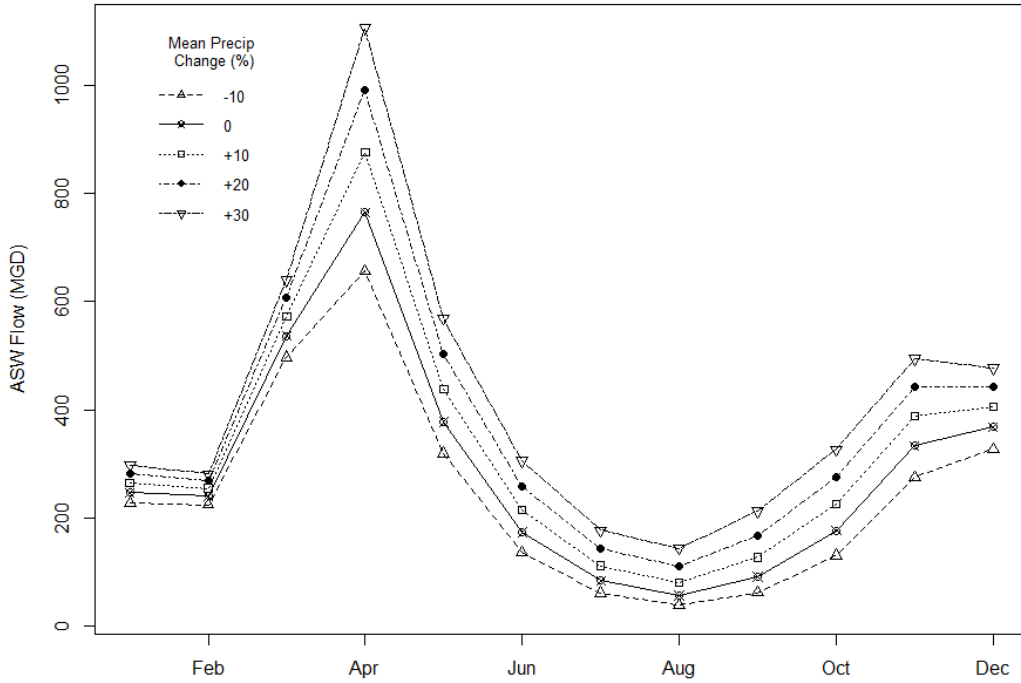
Figure 5. Sensitivity of Ashokan West Inflows to Changes in Precipitation
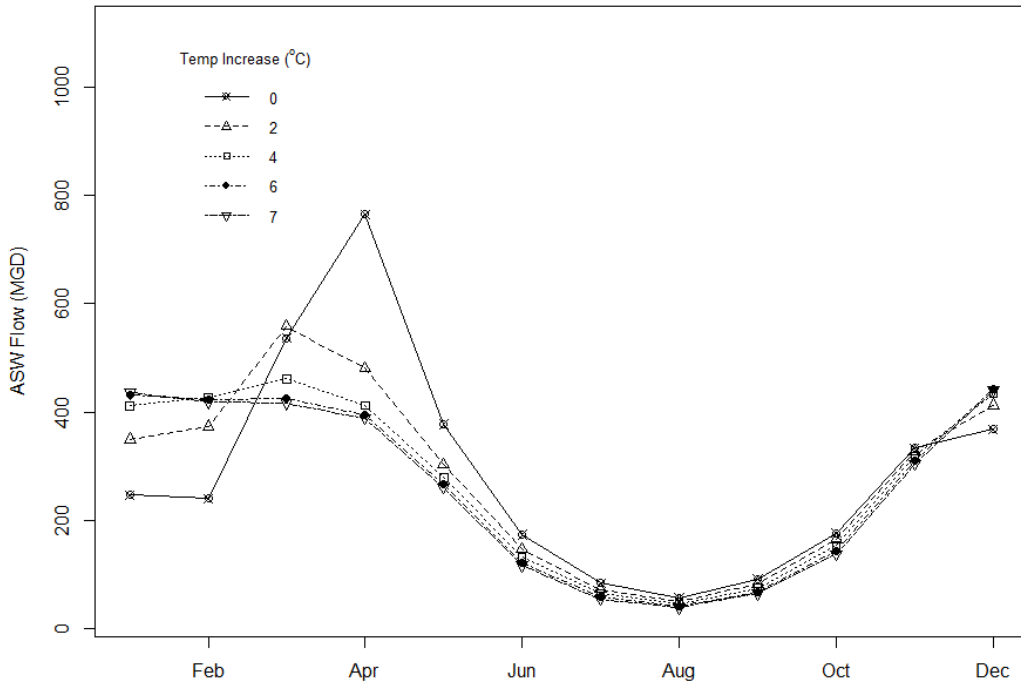
Figure 6. Sensitivity of Ashokan West Inflows to Changes in Temperature

4.2. Climate-altered Turbidity Results

Across all thresholds, the total numbers of turbidity exceedances are sensitive to precipitation (Figures 7, 9, 11, and 13). Increasing precipitation to 130% of the historic mean resulted in as much as a 3-fold increase in turbidity exceedances for peak months in the Ashokan West Reservoir. In Ashokan East, turbidity events in general display a positive correlation with increasing precipitation but there are instances where increased precipitation results in a lower number of exceedances (Figure 13). These departures from the general trend are likely caused by operational decisions, where the increased precipitation across the entire system forces the model to decrease transfers to Ashokan East from Ashokan Westøs highly-turbid water.

Increasing temperatures have a slight inverse relationship with the number of turbidity exceedances across the different thresholds (Figures 8, 10, 12, and 14). In general, both reservoirsø turbidity levels exhibit much less sensitivity to changes in temperature than to changes in precipitation.

While seasonality does not appear to be effected by changes in precipitation, increasing temperatures show changes in monthly trends. The historic high peak months of April and November remain peak months and the typically less-turbid months of February and August continue to experience a low number of events when changes are made to precipitation. Shifts in seasonality can be seen when examining the effects of temperature changes, as increasing temperatures appear to reduce the number of events happening in April and increasing the number of events occurring in the winter months.

Evaluating the effects of changes in temperature and precipitation simultaneously, Ashokan West turbidity exceedances are highly correlated with increased precipitation

and slightly negatively correlated with increasing temperature (Figures 15, 16, 17, and 18). The Ashokan East turbidity exceedances show different trends across months and threshold values (Figures 19, 20, 21, and 22). In general, the peak number of exceedances above 5 NTU in the Ashokan East reservoir seems to be associated with peak precipitation, with an exception in February.

The number of exceedances above 10 NTU in Ashokan East demonstrate a bi-modal behavior due to changes in precipitation, as January through March and August through October all show peak turbidity exceedances occurring when mean precipitation is reduced to 90% of mean. April to July and November and December demonstrate an increasing number of exceedances as precipitation levels increase. Again, these results most likely reflect the ability of the systems model to operate the system to prevent the movement of turbid water Ashokan West and Ashokan East. It should also be noted that, in general, the months showing decreasing exceedances with increasing precipitation are months which experience, on average, a lower number of events than other months.
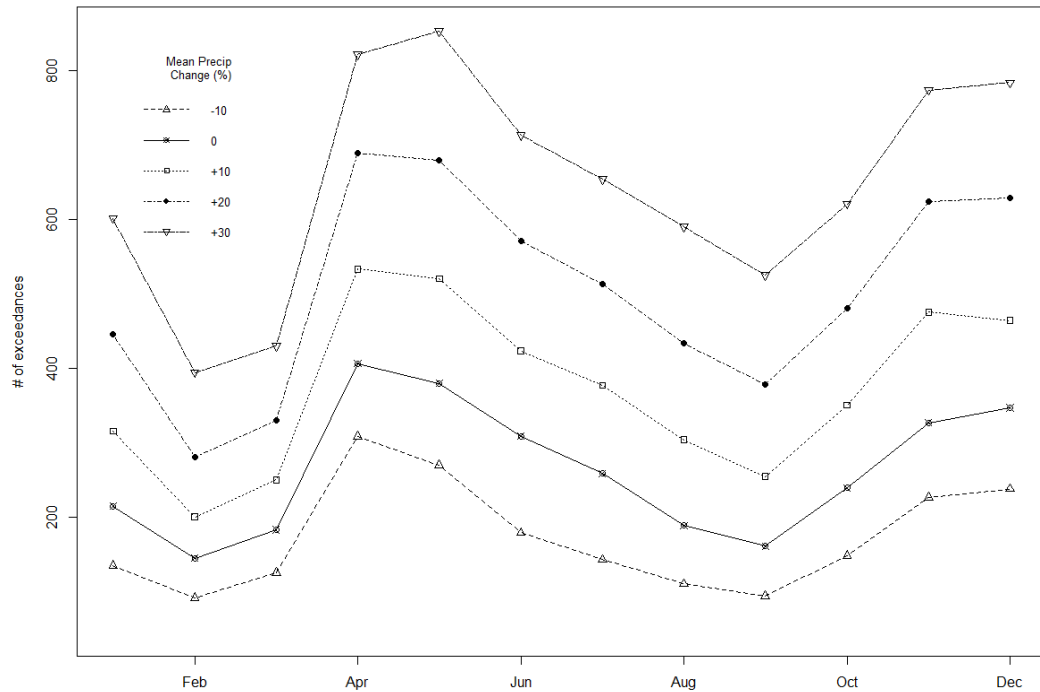
Figure 7. Sensitivity of Ashokan West 10 NTU Threshold to Changes in Precipitation
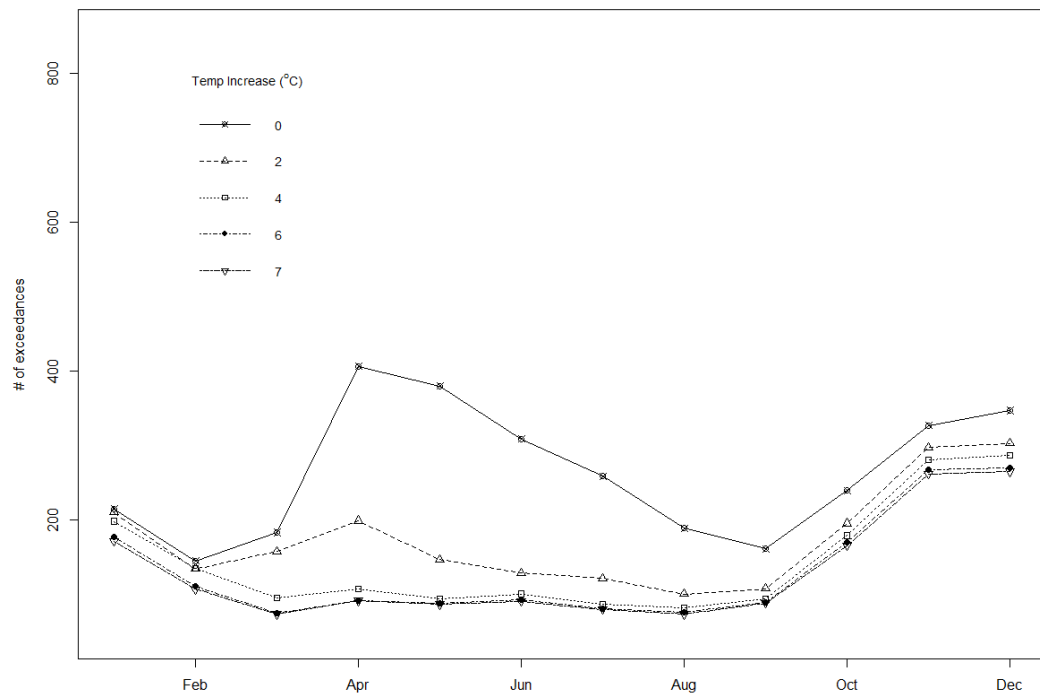
Figure 8. Sensitivity of Ashokan West 10 NTU Threshold to Changes in Temperature
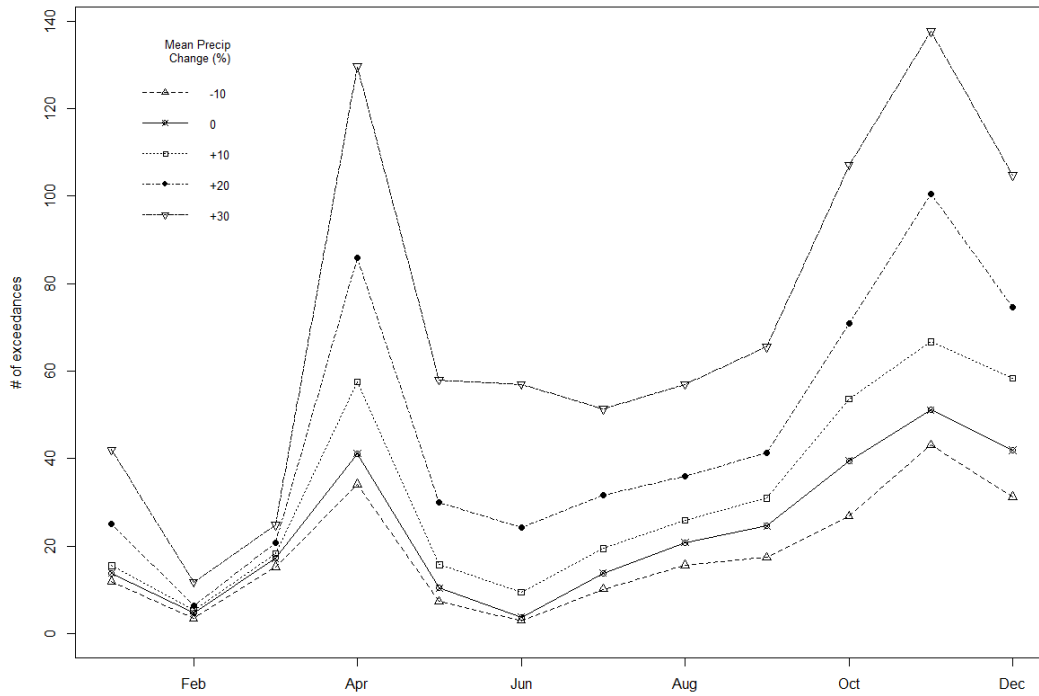
Figure 9. Sensitivity of Ashokan West 25 NTU Threshold to Changes in Precipitation
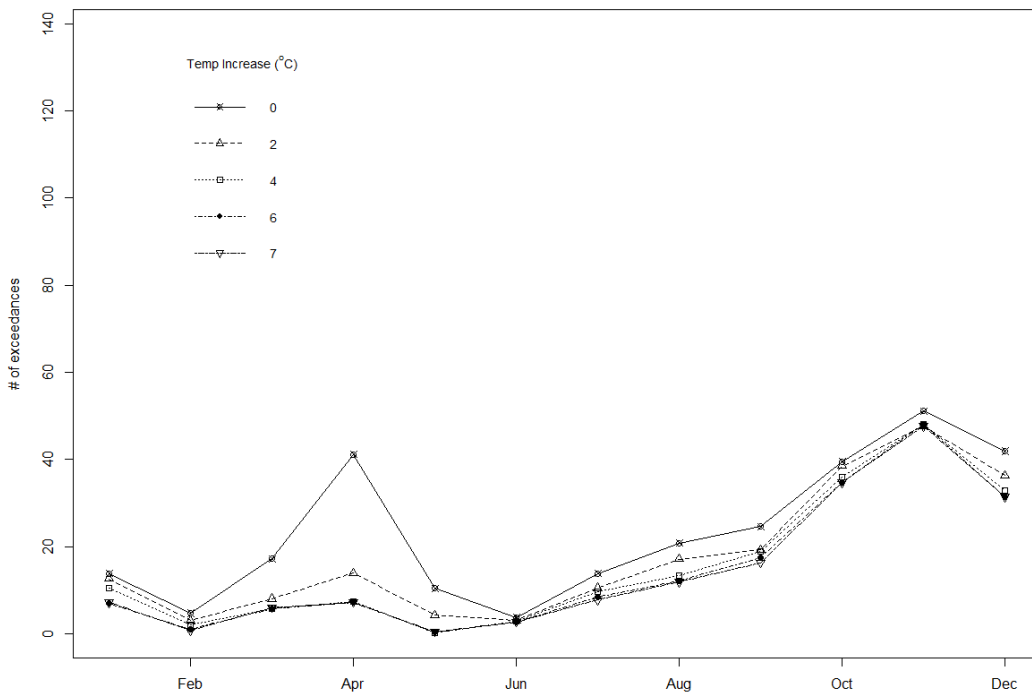
Figure 10. Sensitivity of Ashokan West 25 NTU Threshold to Changes in Temperature
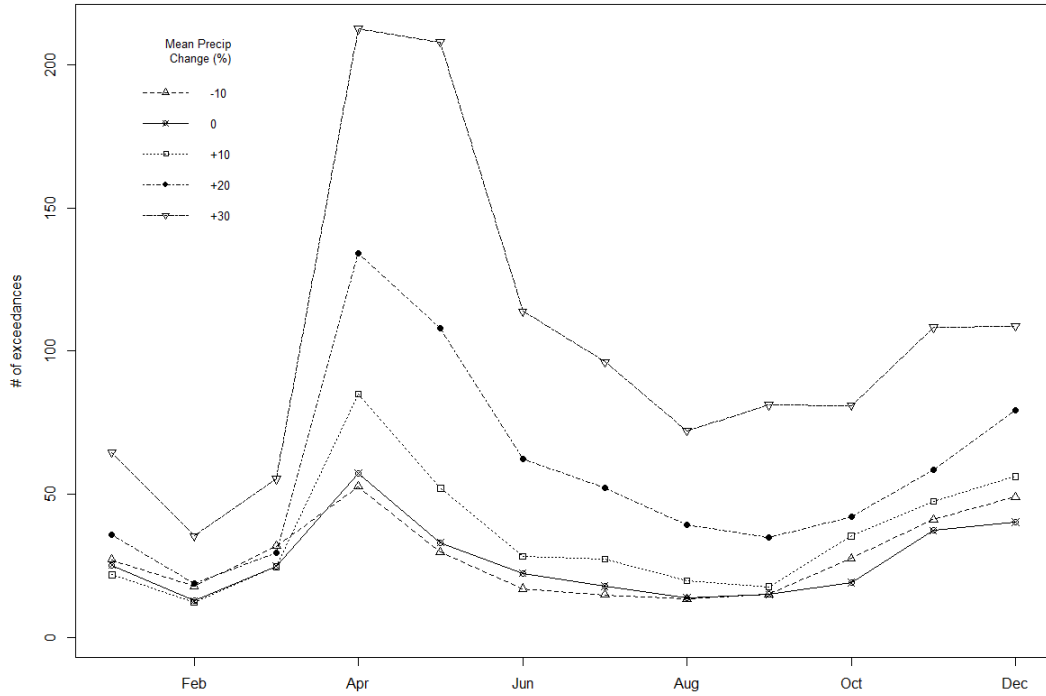
Figure 11. Sensitivity of Ashokan East 5 NTU Threshold to Changes in Precipitation
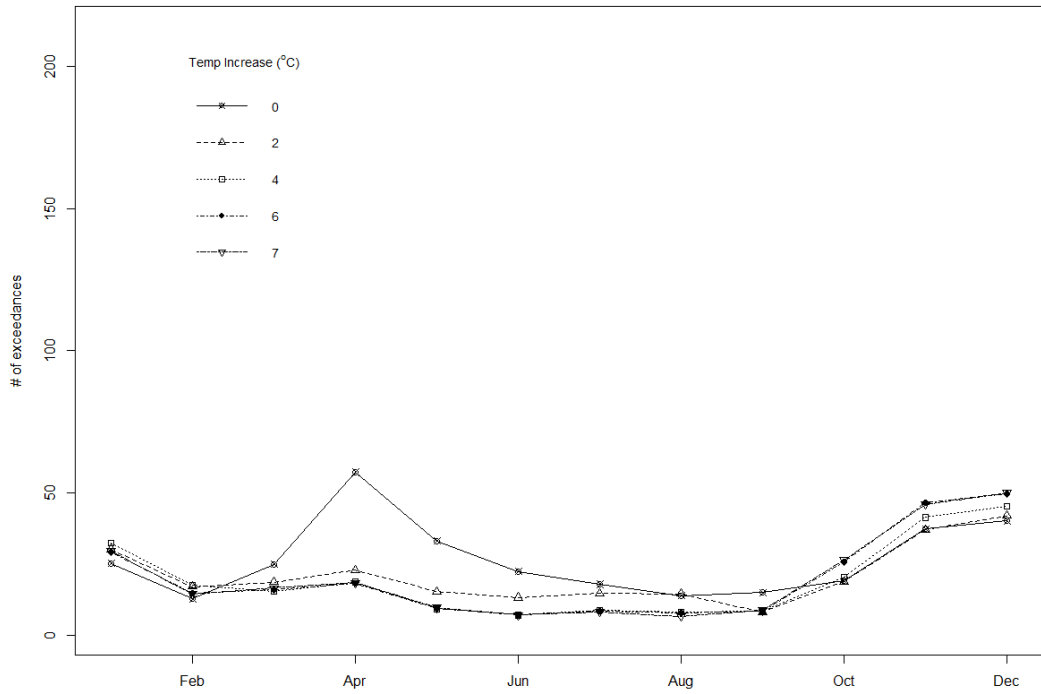
Figure 12. Sensitivity of Ashokan East 5 NTU Threshold to Changes in Temperature
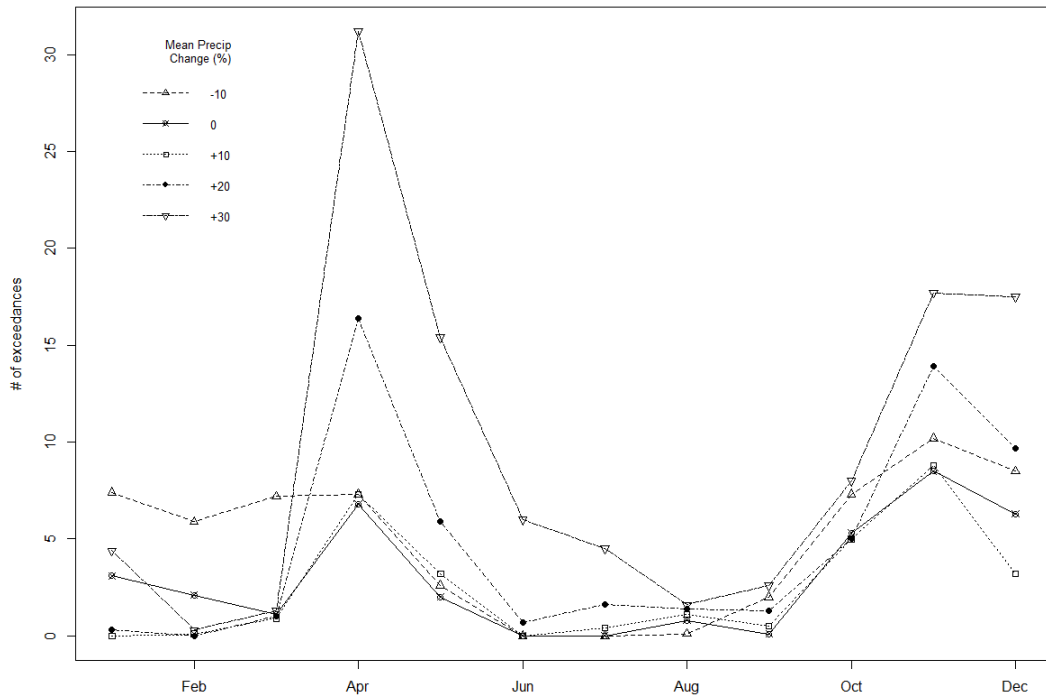
Figure 13. Sensitivity of Ashokan East 10 NTU Threshold to Changes in Precipitation
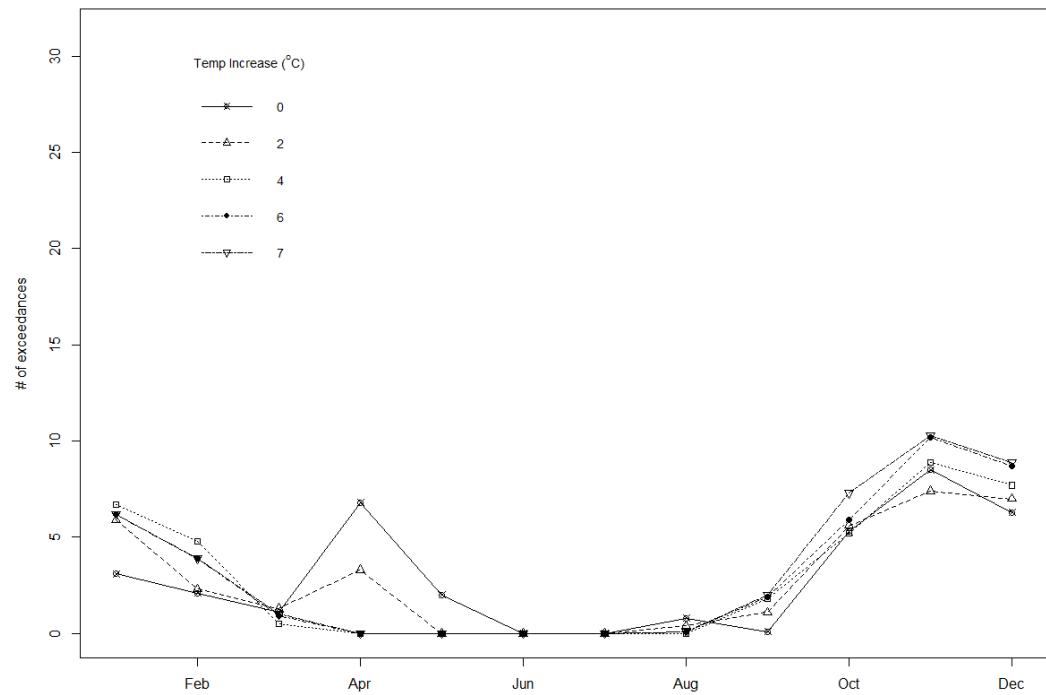
Figure 14. Sensitivity of Ashokan East 10 NTU Threshold to Changes in Temperature
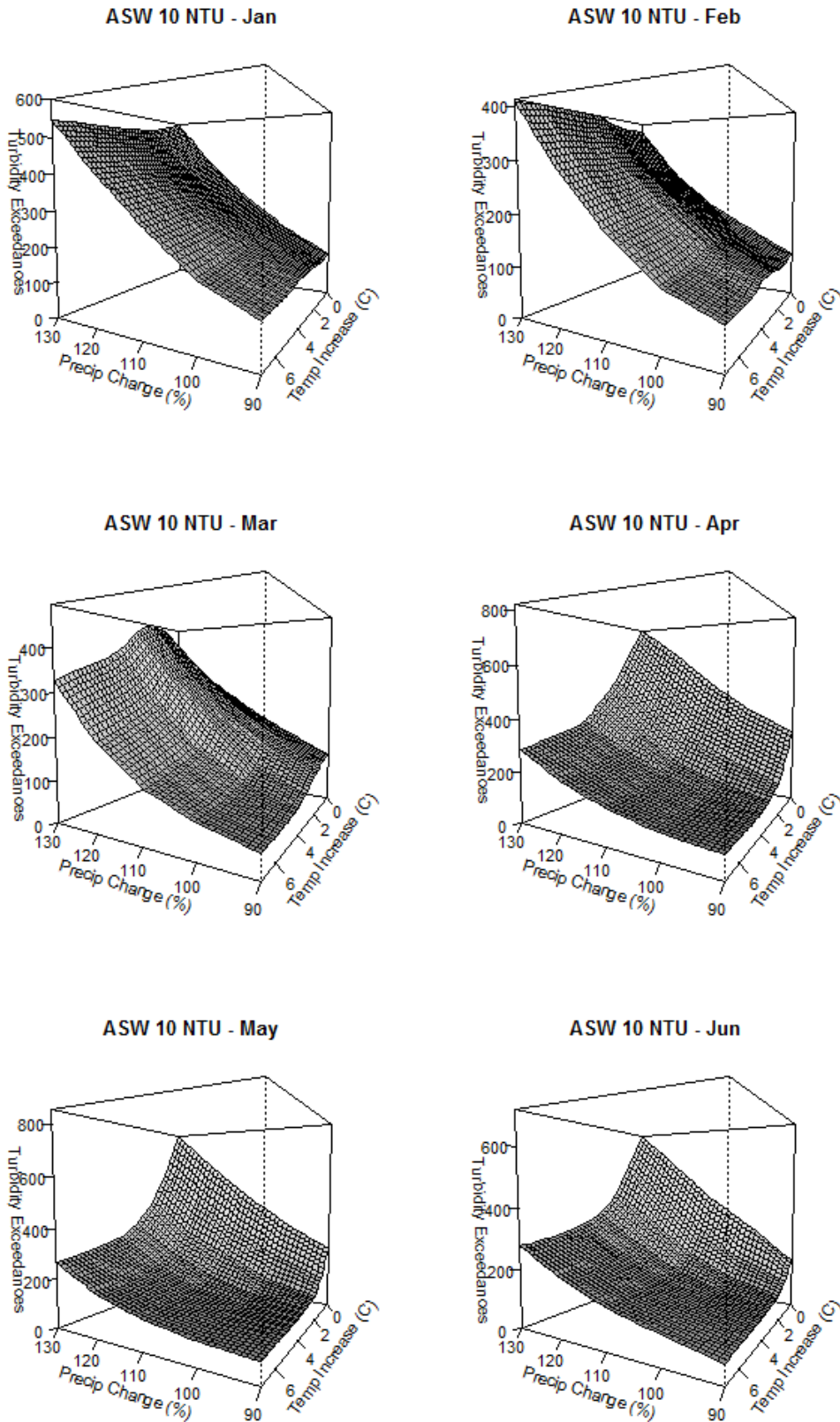
Figure 15. Sensitivity of Ashokan West 10 NTU Threshold to Precipitation and Temperature for January through June
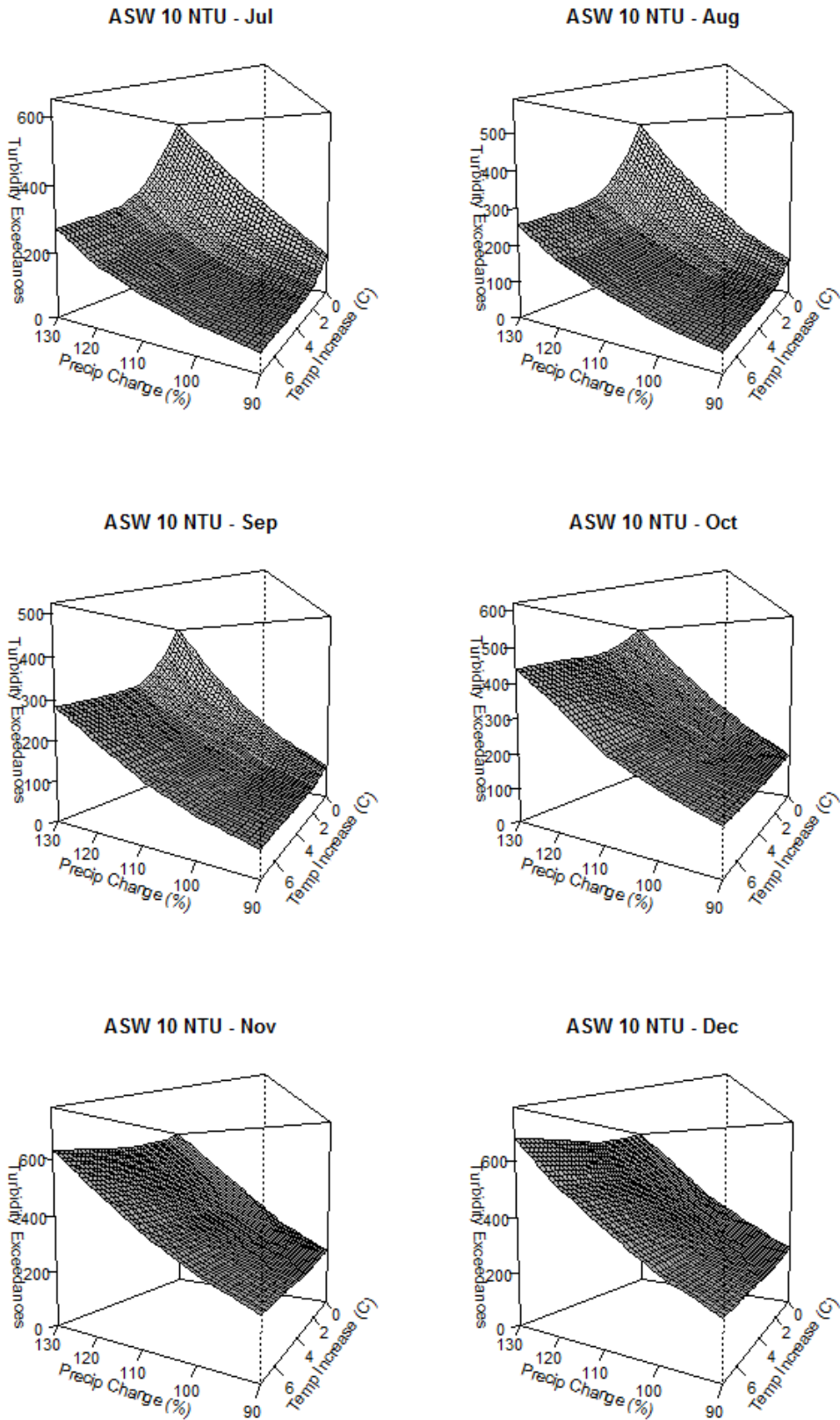
Figure 16. Sensitivity of Ashokan West 10 NTU Threshold to Precipitation and Temperature for July through December
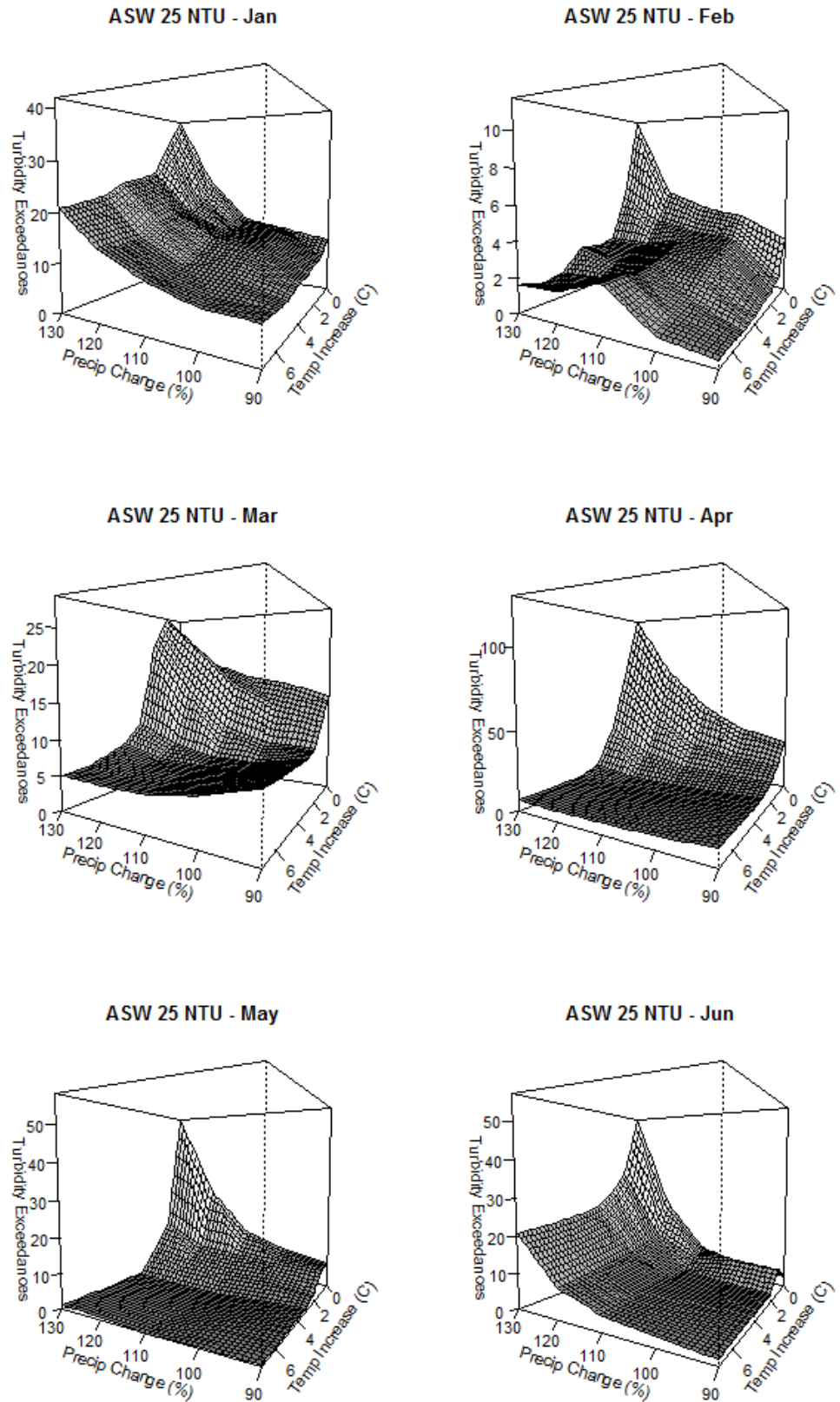
Figure 17. Sensitivity of Ashokan West 25 NTU Threshold to Precipitation and Temperature for January through June
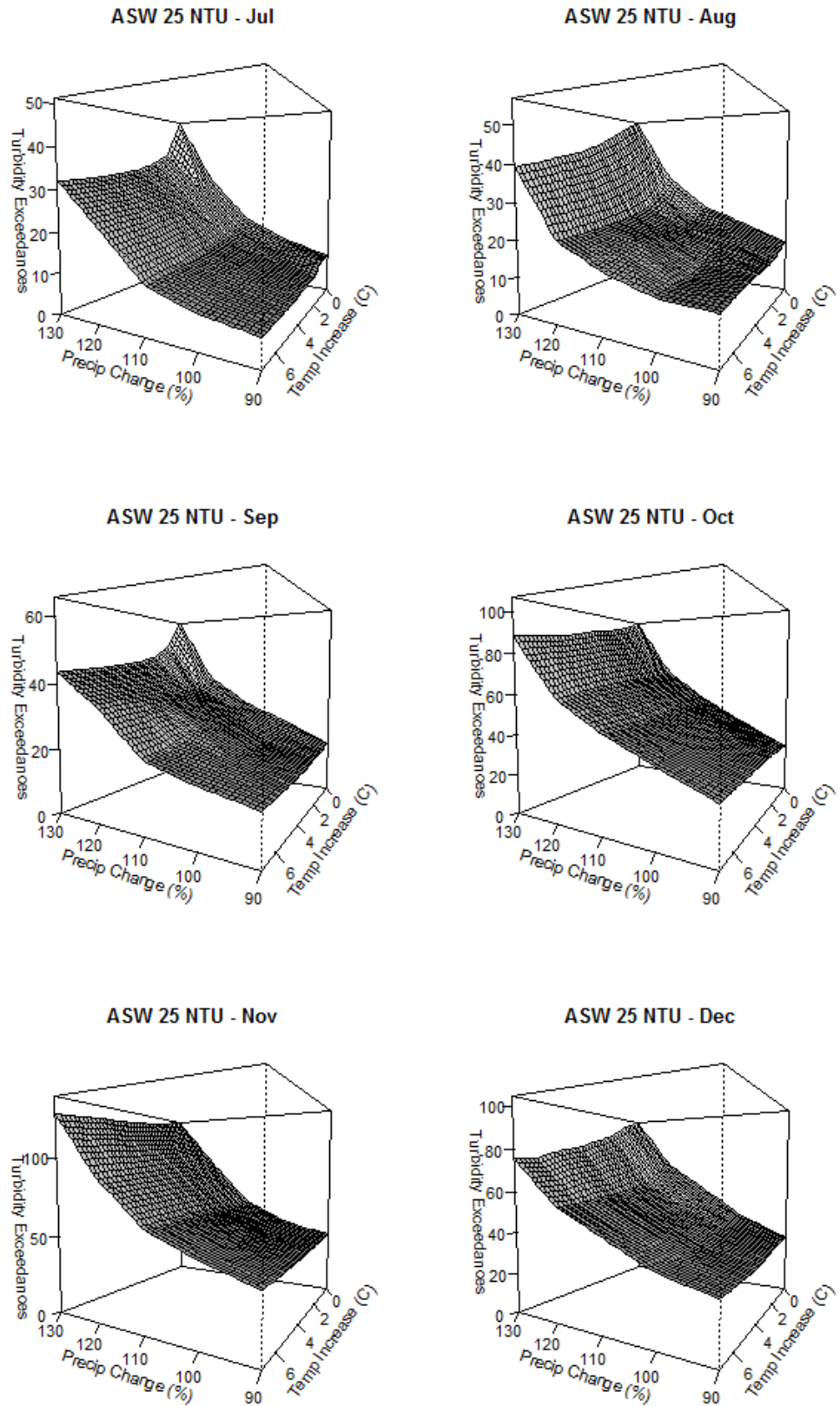
Figure 18. Sensitivity of Ashokan West 25 NTU Threshold to Precipitation and Temperature for July through December
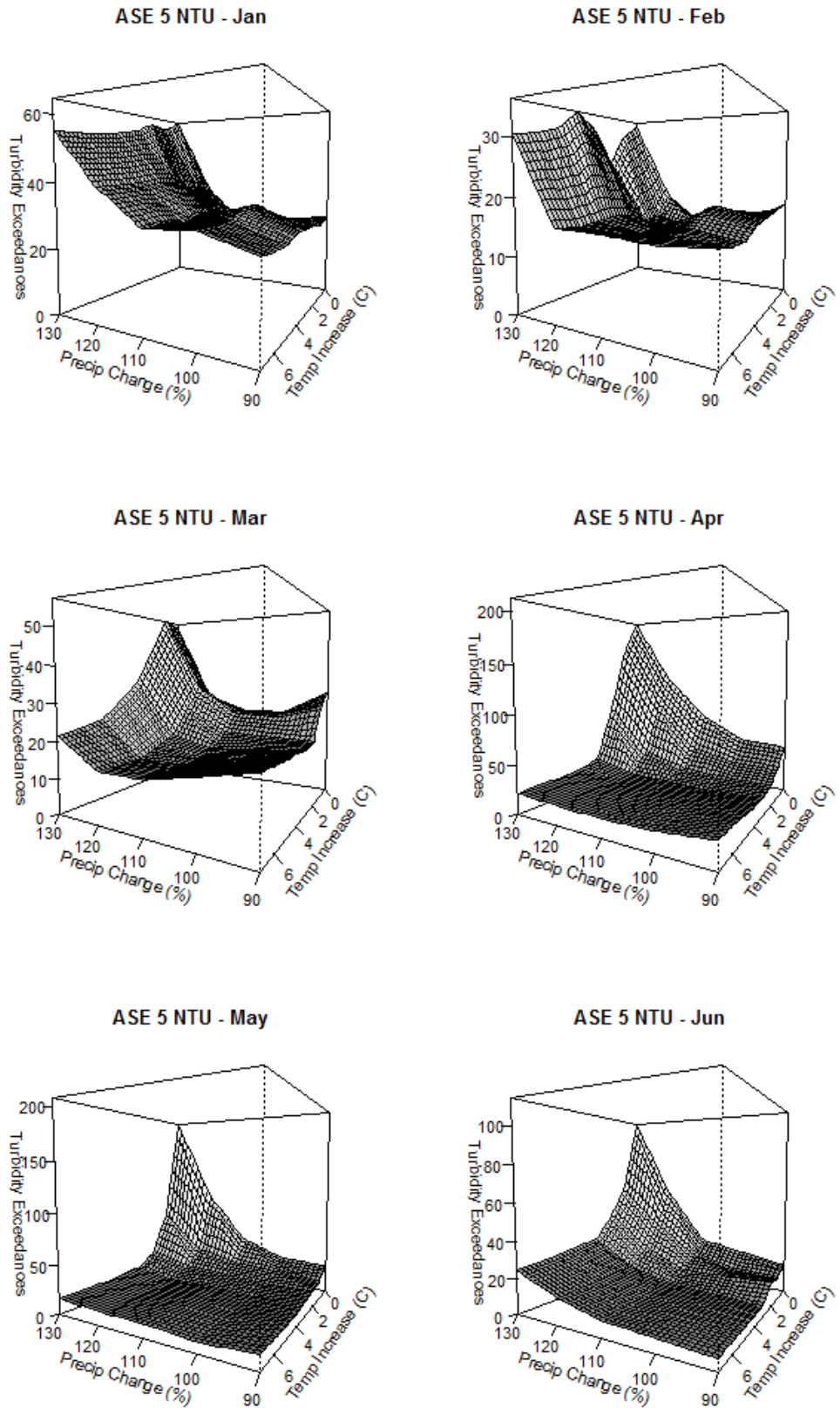
Figure 19. Sensitivity of Ashokan East 5 NTU Threshold to Precipitation and Temperature for January through June
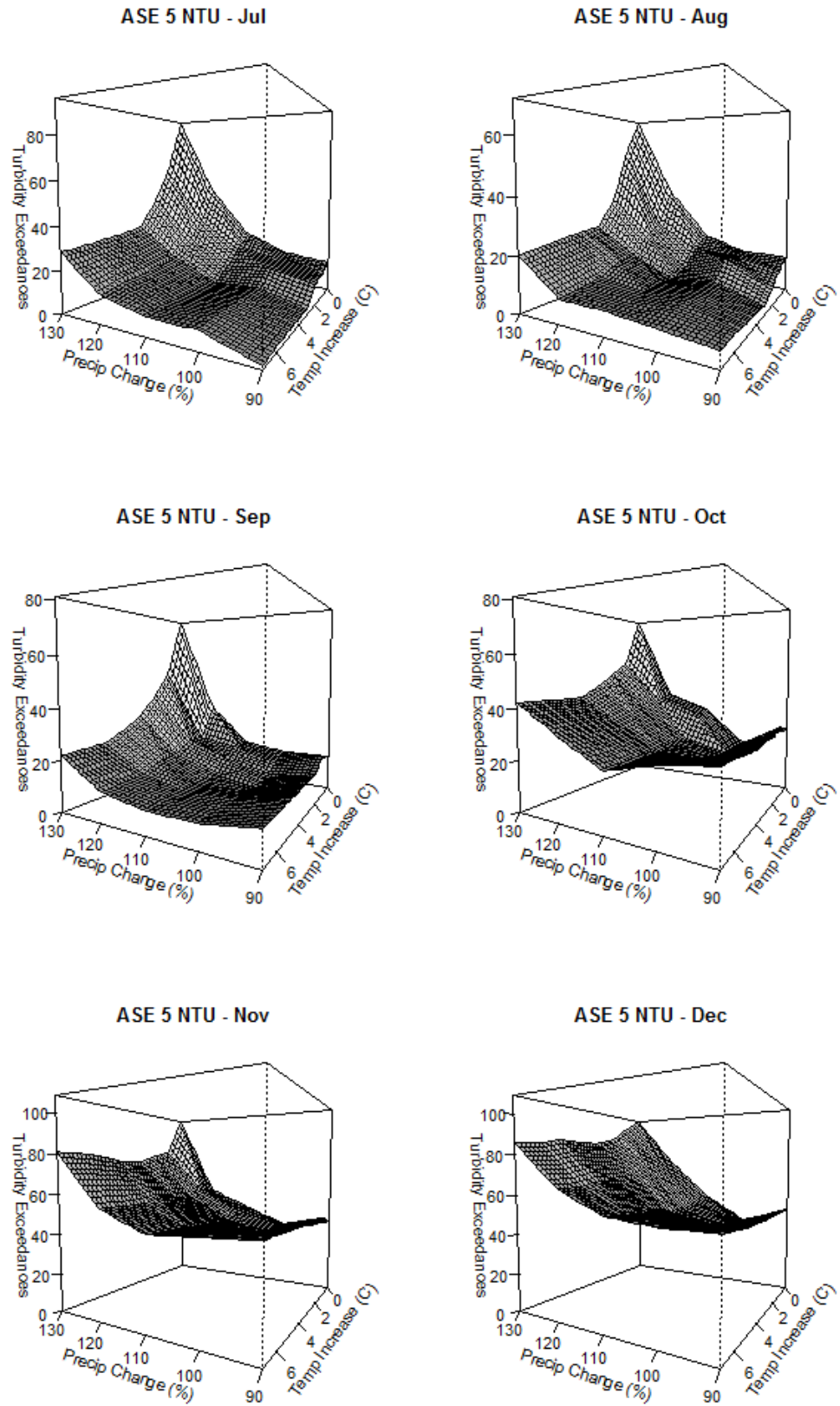
Figure 20. Sensitivity of Ashokan East 5 NTU Threshold to Precipitation and Temperature for July through December
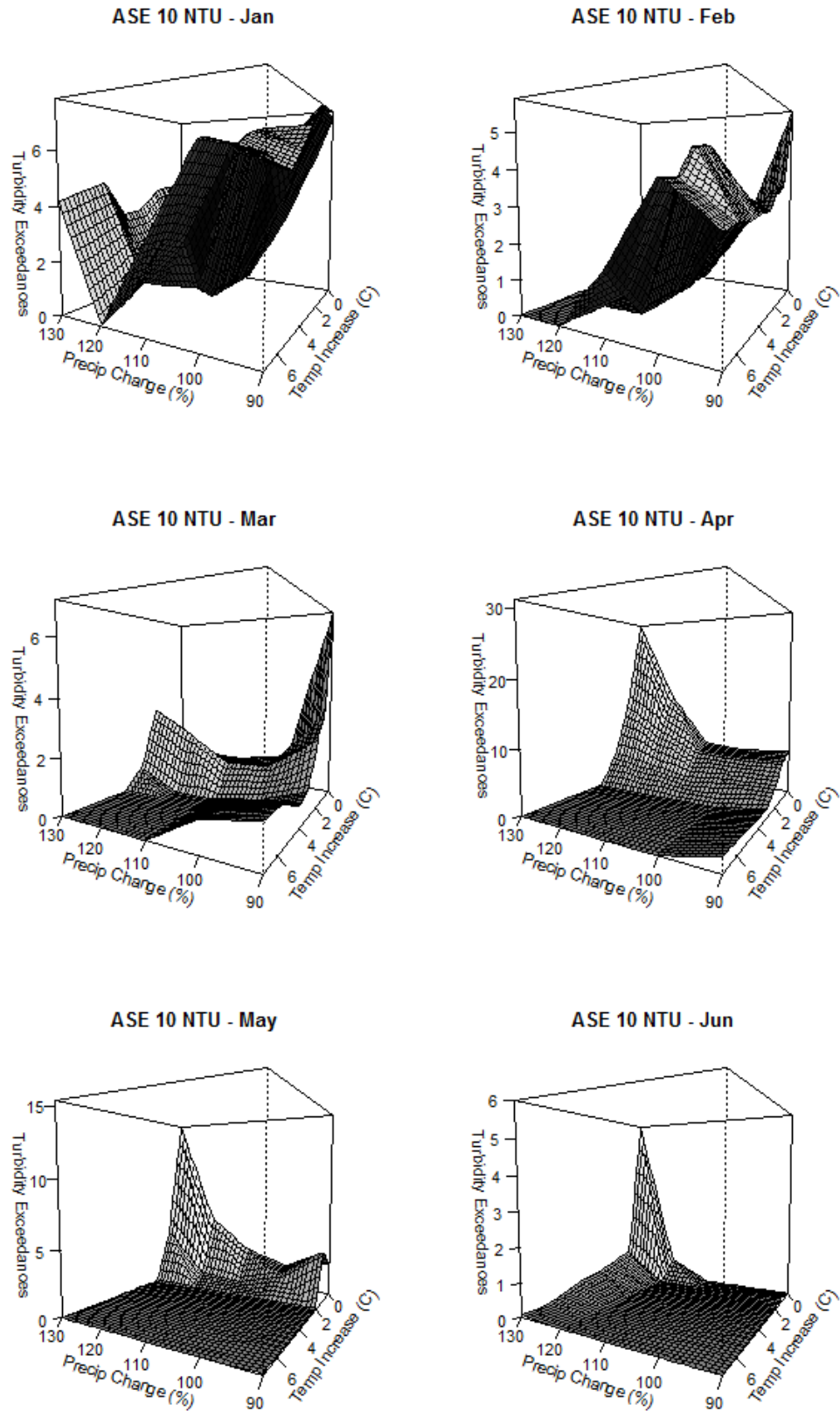
Figure 21. Sensitivity of Ashokan East 10 NTU Threshold to Precipitation and Temperature for January through June
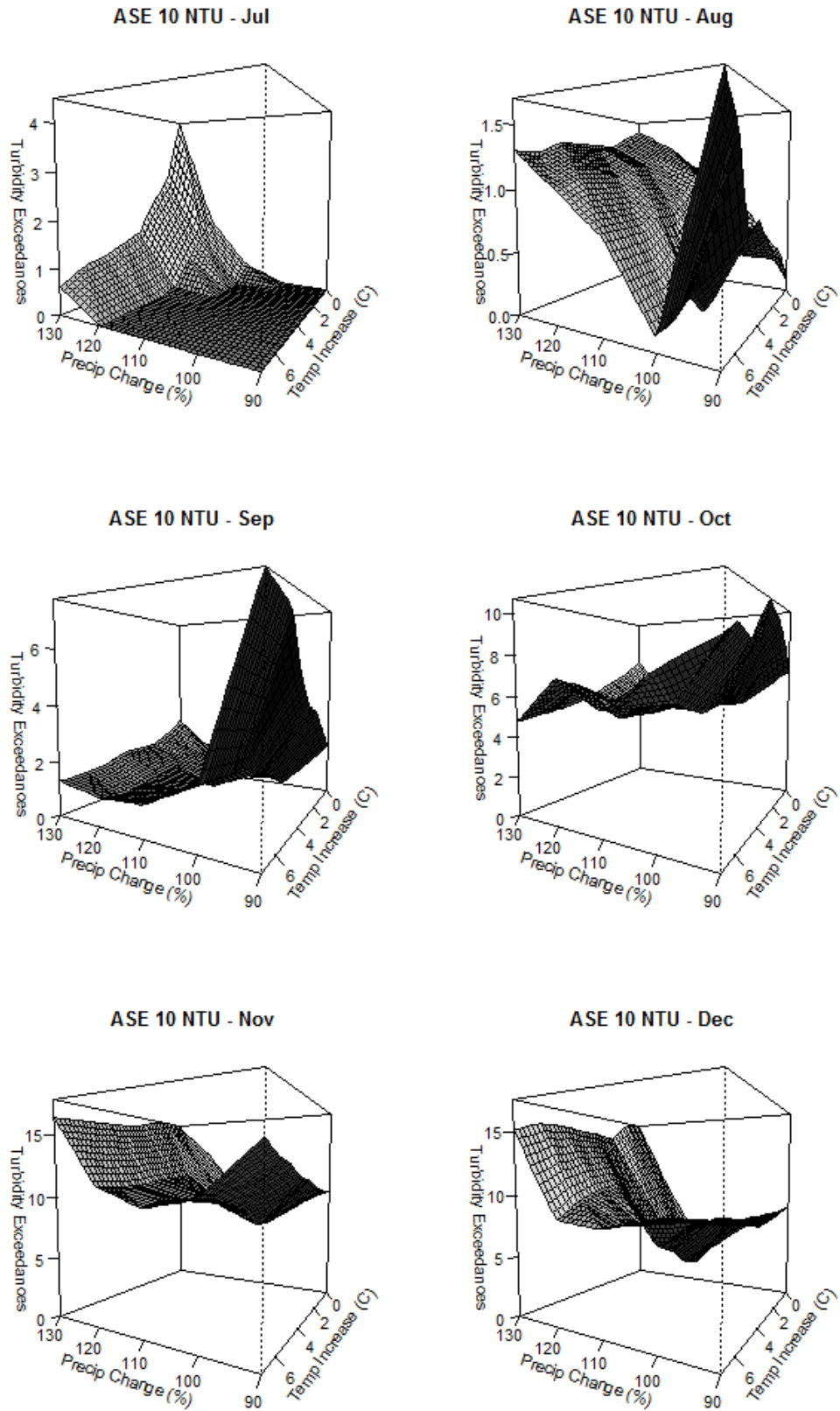
Figure 22. Sensitivity of Ashokan East 10 NTU Threshold to Precipitation and Temperature for July through December

4.3. Operational Effects

The turbidity concentration in the Ashokan East Reservoir is an important consideration for NYCWSS operators when making management decisions. Changes to the number of exceedances above the 5 and 10 NTU thresholds will have significant impacts on the frequency that flow reduction in the Catskill Aqueduct or stop shutter deployment is necessary.

Using the NPCC projections from Section 2.3 and the threshold sensitivities from Appendix B, the total number of threshold exceedances can be estimated and thus the change in frequency of flow reduction measures, including stop shutter usage. Using the ―Middle Range‖ projections for both the 2020s and 2050s, there are temperature increases of approximately 1°C and 3°C, respectively, and precipitation increases of 5% and 10%, respectively. The total number of exceedances for both thresholds and timeslices were estimated (Table 7).

Table 6. Estimated Number of Total Exceedances for Baseline, 2020s, and 2050s

	ASE 5 NTU Threshold Exceedances			ASE 10 NTU Threshold Exceedances		
	Baseline	2020s	2050s	Baseline	2020s	2050s
January	25	20	25	3	2	0
February	14	14	14	2	1.5	0.5
March	25	15	20	1	1	0
April	40	40	10	10	10	5
May	40	40	20	4	2	2
June	30	20	10	0.5	0.5	0.5
July	20	20	10	0.5	0.5	0.5
August	15	15	10	0.8	1	1
September	20	20	10	1	1	1
October	20	30	25	5.5	6	5.5
November	40	50	50	9	9	10
December	45	50	50	4	6	6

Considering the Ashokan East 5 NTU threshold to represent instances when the reservoir operators must reduce flow and the 10 NTU threshold to represent instances when the operators must use stop shutters to further reduce flow, the exceedances estimates give direct insight into the possible changes in frequency of these operations for the 2020s and 2050s.

4.4. Climate and Turbidity Regression

Regression equations were explored to estimate the number of exceedances above the Ashokan West 10 NTU threshold for a 50 year period given changes in precipitation and temperature. Multiple regressions using both precipitation and temperature yielded coefficients for temperature that, on average, had insignificant p-values, resulting in the final form of the regression (Equation 5) which utilized only the squared and cubed values of precipitation. Table 6 contains the coefficient values for use in Equation 5 as well as the resulting correlation between the regressions estimate for total number of exceedances and the model results.

$$ = \quad + \quad + \qquad\qquad\qquad\qquad (5)$$

Where: z = Number of Exceedances over 50 year period
y = Precipitation Change from Mean (%)
β = Coefficient values found in Table 6

Table 7. Regression Coefficients and Correlation Values for Ashokan West 10 NTU Threshold

				R^2
January	0.07	-2.17	485	0.63
February	0.05	-1.62	330	0.62
March	0.06	-1.75	387	0.55
April	0.06	-1.75	675	0.28
May	0.05	-1.67	659	0.26
June	0.05	-1.64	551	0.36
July	0.05	-1.65	504	0.40
August	0.05	-1.48	429	0.43
September	0.05	-1.44	379	0.52
October	0.06	-1.90	493	0.60
November	0.08	-2.39	640	0.62
December	0.08	-2.54	659	0.62

R^2 values range from 0.26 in May to 0.63 in January. Regressions using only the linear and quadratic forms of precipitation resulted in much lower correlation values for this particular threshold. The linear regression had an average R^2 value of 0.22 across all months and the quadratic regression had an average R^2 of 0.27 across all months. This cubic regression showed a significant increase to correlation and as such, the cubic form was chosen to represent the relationship.

This model can be used to accurately predict the number of exceedances above the Ashokan West 10 NTU threshold for any month and change in precipitation or temperature. These predictions can be compared with baseline estimates of exceedances to give operators an idea of the change in exceedances for various levels of climate change. Individual regressions for each month may prove useful moving forward, as the effects of changes in temperature appear to differ depending on the month.

5. CONCLUSIONS

5.1. Comments on Results

Results from the analysis provide insights into the sensitivity of turbidity levels in the Ashokan Reservoir to changes in climate and there are a number of conclusions that can be drawn.

1) The results of this study confirm that turbidity events in the Ashokan West Reservoir will increase in frequency with increasing precipitation. For both the 10 and 25 NTU thresholds, only February and March did not experience consistent increases in total exceedances as precipitation was increased. Generally, the proportion of increases month-to-month is similar, with no single month effected by increasing precipitation more than others.

2) Temperature increases will decrease the number of turbidity events in the Ashokan West Reservoir and can be a more powerful driver of the total number of events than precipitation in some months. The results of this analysis show a general decline in the total number of exceedances with increasing temperature for all months for both 10 and 25 NTU threshold values. Some months are more effected by changes in temperature than others, as increasing temperature is shown to drastically decrease the number of events in the peak month of April while only slightly decreasing the number of events in January. This is likely because of higher temperature causing precipitation in the winter to fall as rain, reducing snowpack runoff in the spring.

3) Increasing precipitation will generally increase the number of turbidity exceedances above 5 NTU in the Ashokan East Reservoir, though some months do not show a consistent positive relationship, such as March. Temperature appears to be very

negatively correlated with turbidity exceedances above 5 NTU, with peak exceedances occurring at mean temperature for all months.

4) Exceedances of the 10 NTU turbidity threshold in the Ashokan East Reservoir appear more random than the other exceedances metrics tested. It appears that the ability of operators to make decisions that keep the concentration low play a crucial part in the number of exceedances. For instance, in January, the total number of exceedances decreases as precipitation approaches 120% of mean, and then bounces back and rises as it approaches 130% of mean. The operational decisions that allowed the number of exceedances to fall as precipitation approached 120% may be useful to the NYCDEP, as well as understanding what caused the turbidity to rise immediately after that level of precipitation was crossed.

5) From January to September, the number of times that operators must reduce flow because of high turbidity concentrations is either reduced or unchanged for both the 2020s and 2050s. From October to December, that number is increasing or unchanged for both time slices. These changes to the frequency of flow reduction are likely caused by the projection's moderate increases to temperature compared to the slight increases in precipitation. As seen in the results portion, higher temperatures tend to increase the number of exceedances in the colder months and decrease in other parts of the year because of the increased flows in the winter and decrease of snowpack throughout the rest of the year.

6) The number of times that stop shutters are used appears to follow the same general trend as flow reduction measures for the 2020s and 2050s. From January to September the frequency is decreasing or remaining neutral, from October to December,

the frequency increases. Again, this change in frequency is likely caused by the increased temperature in these scenarios and the subsequent changes to the seasonality of inflows, as seen in Section 4.1.

5.2. Revisiting Objectives

This thesis used a Decision-Scaling style framework to evaluate the sensitivity of Ashokan Reservoir turbidity to changes in climate. To do this, time-series of precipitation and temperature were generated that captured the historic data's trends but also altered the annual means of precipitation and temperature. These time-series allowed for the testing of the GWLF hydrology model and STATS simulation model under a wide range of climate scenarios. This sensitivity analysis gives important insight to the NYCDEP regarding how their system responds to change. The results of the testing were analyzed and the responses of the system to changes in climate were well-catalogued and cross-examined with the latest climate projections to estimate the changes in operations that the NYCWSS may experience under future climate scenarios. In the future, other metrics of interests can be explored in the same fashion that this study explored the total number of turbidity threshold exceedances to give further insight into the response of the NYCWSS to changes in climate.

REFERENCES

Alcott, E., Ashton, M. S., & Gentry, B. S. (2013). *Natural and Engineered Solutions for Drinking Water Supplies*. Boca Raton, FL: Taylor & Francis.

Brown, C., Ghile, Y., Laverty, M., & Li, K. (2012). Decision scaling: Linking bottom-up vulnerability analysis with climate projections in the water sector. *Water Resources Research*, *48*(9). doi:10.1029/2011WR011212

Brown, C., Werick, W., Leger, W., & Fay, D. (2011). A Decision-Analytic Approach to Managing Climate Risks: Application to the Upper Great Lakes1. *JAWRA Journal of the American Water Resources Association*, *47*(3), 524ó534. doi:10.1111/j.1752-1688.2011.00552.x

Brown, C., & Wilby, R. L. (2012). An Alternate Approach to Assessing Climate Risks. *EOS*, *92*(41), 92ó94.

Christensen, N. S., Wood, A. W., Voisin, N., Lettenmaier, D. P., & Palmer, R. N. (2004). The Effects of Climate Change on the Hydrology and Water Resources of the Colorado River Basin. *Climatic Change*, *62*, 337ó363.

Cole, T. M., Buchak, E. M., & J.E. Edinger Associates, I. (1995). *CE-QUAL-W2: A Two-Dimensional Laterally Averaged, Hydrodynamic and Water Quality Model, Version 2.0.*

Dessai, S., & Hulme, M. (2004). Does climate adaptation policy need probabilities? *Climate Policy*, *4*(2), 107ó128. doi:10.3763/cpol.2004.0411

DeCristofaro, L. (2014). Calibration and Verification of STATS. UMass Amherst and NYCDEP communications, April 2014.

Effler, S. W., Perkins, M. G., Ohrazda, N., Brooks, C. M., & Wagner, B. A. (1998). Turbidity and Particle Signatures Imparted by Runoff Events in Ashokan Reservoir, NY. *Journal of Lake and Reservoir Management*, *14*, 254ó265.

Gelda, R. K., Effler, S. W., Peng, F., Owens, E. M., & Pierson, D. C. (2009). Turbidity Model for Ashokan Reservoir , New York : Case Study. *Journal of Environmental Engineering*, *135*, 885ó895.

Guzman, J. R. and Lund, J. (1999). Derived Operating Rules for Reservoir in Series or in Parallel. *Journal of Water Resources Planning and Management*, *125*(3), 143ó153.

Haith, D., & Shoemaker, L. (1987). Generalized Watershed Loading Functions for Streamflow Nutrients. *Water Resources Bulletin*, *23*, 471 ó 478.

Horton, R. M., Gornitz, V., Bader, D. a., Ruane, A. C., Goldberg, R., & Rosenzweig, C. (2011). Climate Hazard Assessment for Stakeholder Adaptation Planning in New York City. *Journal of Applied Meteorology and Climatology*, *50*(11), 2247‚2266. doi:10.1175/2011JAMC2521.1

HydroLogics Inc. (2007). *User Manual for OASIS with OCL*. Columbia, MD.

Intergovernmental Panel on Climate Change (2012). *Managing the Risks of Extreme Events and Disasters to Advance Climate Change Adaptation. A Special Report of Working Groups I and II of the Intergovernmental Panel on Climate Change* [Field, C.B., V. Barros, T.F. Stocker, D. Qin, D.J. Dokken, K.L. Ebi, M.D. Mastrandrea, K.J. Mach, G.-K. Plattner, S.K. Allen, M. Tignor, and P.M. Midgley (eds.)]. Cambridge University Press, Cambridge, UK, and New York, NY, USA, 582 pp.

Jones, R. N. (2001). An Environmental Risk Assessment / Management Framework for Climate Change Impact Assessments. *Natural Hazards*, *23*, 197‚230.

Kiparsky, M., Milman, A., & Vicuña, S. (2012). Climate and Water: Knowledge of Impacts to Action on Adaptation. *Annual Review of Environment and Resources*, *37*(1), 163‚194. doi:10.1146/annurev-environ-050311-093931

Kundzewicz, Z. W., & Stakhiv, E. Z. (2010). Are climate models õready for prime timeö in water resources management applications, or is more research needed? *Hydrological Sciences Journal*, *55*(7), 1085‚1089. doi:10.1080/02626667.2010.513211

Lempert, R., Nakicenovic, N., Sarewitz, D., & Schlesinger, M. (2004). Characterizing climate-change uncertainties for decision-makers. *Climatic Change*, *65*, 1‚9.

Matonse, A. H., Pierson, D. C., Frei, A., Zion, M. S., Anandhi, A., Schneiderman, E., & Wright, B. (2012). Investigating the impact of climate change on New York Cityøs primary water supply. *Climatic Change*, *116*(3-4), 437‚456. doi:10.1007/s10584-012-0515-4

Matonse, A. H., Pierson, D. C., Frei, A., Zion, M. S., Schneiderman, E. M., Anandhi, A., Pradhanang, S. M. (2011). Effects of changes in snow pattern and the timing of runoff on NYC water supply system. *Hydrological Processes*, *25*(21), 3278‚3288. doi:10.1002/hyp.8121

Maurer, E. P., A. W. Wood, J. C. Adam, D. P. Lettenmaier, and B. Nijssen (2002), A long-term hydrologically-based data set of land surface fluxes and states for the conterminous United States, *J. Clim*., 15, 3237ó3251.

Milly, P. C. D., Betancourt, J., Falkenmark, M., Hirsch, R. M., Zbigniew, W., Lettenmaier, D. P., & Stouffer, R. J. (2008). Stationarity Is Dead : Whither Water Management ? *Science*, *319*(February), 573ó574.

Moody, P., & Brown, C. (2012). Modeling stakeholder-defined climate risk on the Upper Great Lakes. *Water Resources Research*, *48*(10). doi:10.1029/2012WR012497

Mukundan, R., Pierson, D. C., Schneiderman, E. M., OøDonnell, D. M., Pradhanang, S. M., Zion, M. S., & Matonse, a. H. (2013). Factors affecting storm event turbidity in a New York City water supply stream. *Catena*, *107*, 80ó88. doi:10.1016/j.catena.2013.02.002

Nagle, G. N., Fahey, T. J., Ritchie, J. C., & Woodbury, P. B. (2007). Variations in sediment sources and yields in the Finger Lakes and Catskills regions of New York. *Hydrological Processes*. doi:10.1002/hyp

Nash, J. E., & J.V., Sutcliffe. (1970). River Flow Forecasting Through Conceptual Models: Part 1. A Discussion of Principles. *Journal of Hydrology*, *10*, 282 ó 290.

New York City Department of Environmental Protection (2007). New York Cityøs Water Supply System Map. Retrieved from http://www.nyc.gov/html/dep/html/drinking_water/wsmaps_wide.shtml

New York City Department of Environmental Protection (2008). *Report 1: Assessment and Action Plan – A Report Based on the Ongoing Work of the DEP Climate Change Task Force. The New York City Department of Environmental Protection Climate Change Program. DEP with contributions by Columbia University Center for Climate Systems Research and HydroQual Environmental Engineers & Scientists, P.C.,* New York, NY

New York City Department of Environmental Protection. (2010). New York Cityøs Operations Support Tool (OST) White Paper Prepared for The Delaware River Basin Supreme Court Decree Parties. Retrieved from http://water.usgs.gov/osw/odrm/documents/OST_White_Paper.pdf

New York City Department of Environmental Protection. (2011). Water System Safe Yield   Calculation ó 2011. Retrieved from http://www.nyc.gov/html/dep/pdf/ffmp/water_system_safe_yield_calculation_2011.pdf

New York City Department of Environmental Protection. (2012). New York City 2012 Drinking Water Supply and Quality Report. Retrieved from http://www.nyc.gov/html/dep/pdf/wsstate12.pdf

New York City Department of Environmental Protection. (2014a). History of New York City's Water Supply System. Retrieved from http://www.nyc.gov/html/dep/html/drinking_water/history.shtml

New York City Department of Environmental Protection. (2014b). Ashokan. Retrieved from http://www.nyc.gov/html/dep/html/watershed_protection/ashokan.shtml

New York City Panel on Climate Change (2013). *Climate Risk Information 2013: Observations, Climate Change Projections, and Maps*. [C. Rosenzweig and W. Solecki (Editors)]. New York, New York.

R Core Team (2012). R: A language and environment for statistical computing. R Foundation for Statistical Computing, Vienna, Austria. ISBN 3-900051-07-0, URL: http://www.R-project.org/.

Safe Drinking Water Act of 1974, Pub. L. No. 93-523, § 300f, 88 Stat. 1660 (1974)

Samal, N. R., Matonse, A. H., Mukundan, R., Zion, M. S., Pierson, D. C., Gelda, R. K., & Schneiderman, E. M. (2013). Modelling potential effects of climate change on winter turbidity loading in the Ashokan Reservoir, NY. *Hydrological Processes*, *27*(21), 3061ó3074. doi:10.1002/hyp.9910

Schneiderman, E. M., Pierson, D. C., Lounsbury, D. G., & Zion, M. S. (2003). Modeling the Hydrochemistry of the Cannonsville Watershed with Generalized Watershed Loading Functions (GWLF) 1. *Journal of The American Water Resources Association*, *38*(5), 1323ó1347.

Schneiderman, E. M., Steenhuis, T. S., Thongs, D. J., Easton, Z. M., Zion, M. S., Neal, A. L., Walter, M. T. (2007). Incorporating variable source area hydrology into a curve-number-based watershed model. *Hydrological Processes*, *21*, 3420ó3430. doi:10.1002/hyp

Stakhiv, E. Z. (2011). Pragmatic Approaches for Water Management Under Climate Change Uncertainty1. *JAWRA Journal of the American Water Resources Association*, *47*(6), 1183ó1196. doi:10.1111/j.1752-1688.2011.00589.x

Steinschneider, S., & Brown, C. (2013). A semiparametric multivariate, multisite weather generator with low-frequency variability for use in climate risk assessments. *Water Resources Research*, *49*(11), 7205ó7220. doi:10.1002/wrcr.20528

Thomann, R. v. (1982). Verification of Water Quality Models. *Journal of Environmental Engineering*, *108*(5), 923 ó 940.

Thomas, H. A., & Fiering, M. B. (1962). The Mathematical Synthesis of Streamflow Sequences. *Design of Water-Resources Systems*, 459 ó 493.

USGCRP (2013). National Climate Assessment, Public Review Version, Retrieved from http://ncadac.globalchange.gov/.

Ventana System, Inc. (2013). Vensim DSS. http://www.vensim.com/.

Water Utility Climate Alliance. (2010). Decision Support Planning Methods: Incorporating Climate Change Uncertainties Into Water Planning.

Water Utility Climate Alliance. (2009). Options for Improving Climate Modeling to Assist Water Utility Planning for Climate Change.

Wilby, R. L., Charles, S. P., Zorita, E., Timbal, B., Whetton, P., & Mearns, L. O. (2004). Guidelines for Use of Climate Scenarios Developed from Statistical Downscaling Methods. *IPCC Supporting Material*, (August), 1ó27.

Wiley, M. W., & Palmer, R. N. (2008). Estimating the Impacts and Uncertainty of Climate Change on a Municipal Water Supply System. *Journal of Water Resources Planning and Management*, *134*, 239ó246.

Wolman, M. G., & Miller, J. P. (1960). Magnitude and Frequency of Forces in Geomorphic Processes. *The Journal of Geography*, *68*(1), 54ó74.

APPENDIX A

LIST OF REGULATIONS USED IN STATS

Supreme Court Decree 1954

Flexible Flow Management Program Agreement(s) ô June 1, 2012 and June 1, 2013

New York State Department of Environmental Conservation/New York City Department of Environmental Protection (DEC/DEP) Interim Ashokan Release Protocol. ô October 18, 2011

New York City's Operations Support Tool (OST) White Paper Prepared for The Delaware River Basin Supreme Court Decree Parties. ô October 8, 2010

New York State Department of Environmental Protection Regulations: Chapter X,
Part 670: Reservoir Releases Regulations: Schoharie Reservoir Shandaken Tunnel-Esopus Creek
Part 671: Reservoir Releases Regulations: Cannonsville, Pepacton and Neversink Reservoirs
Part 672: Reservoir Releases Regulations: Other
Subpart 672-1: Reservoir Releases Regulations ó General
Subpart 672-2: Ashokan, Kensico, Rondout and Schoharie Reservoirs

APPENDIX B

THRESHOLD EXCEEDANCE CONTOURS

ASW 10 NTU - Jan

ASW 10 NTU - Feb

ASW 10 NTU - Mar

ASW 10 NTU - Apr

ASW 10 NTU - May
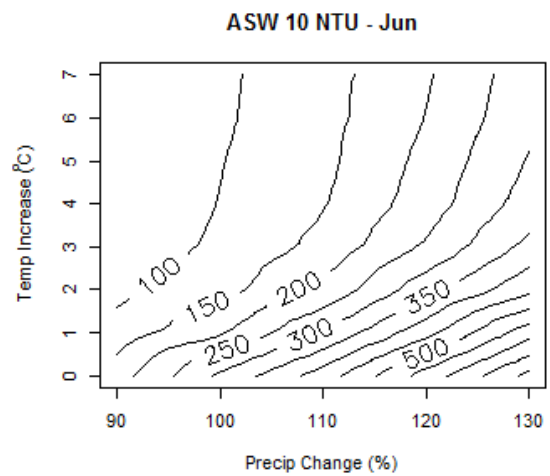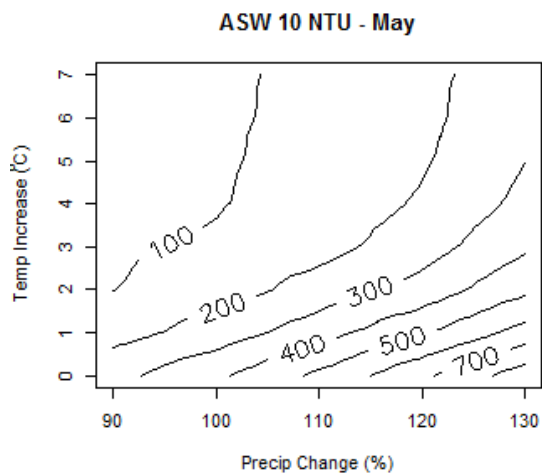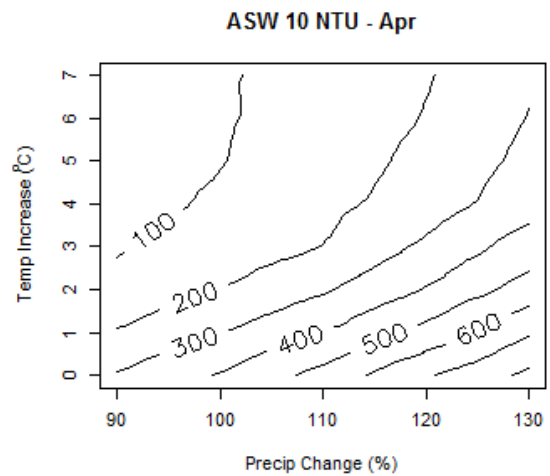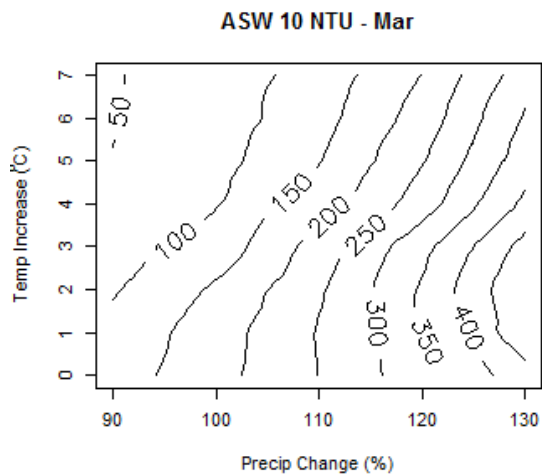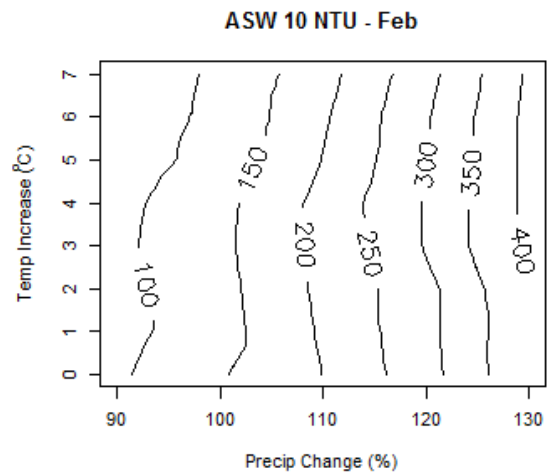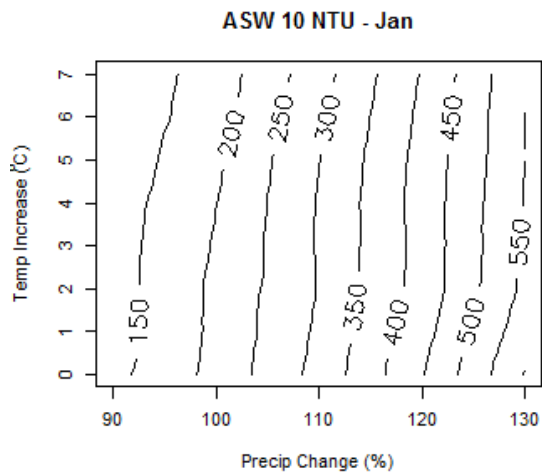
ASW 10 NTU - Jun
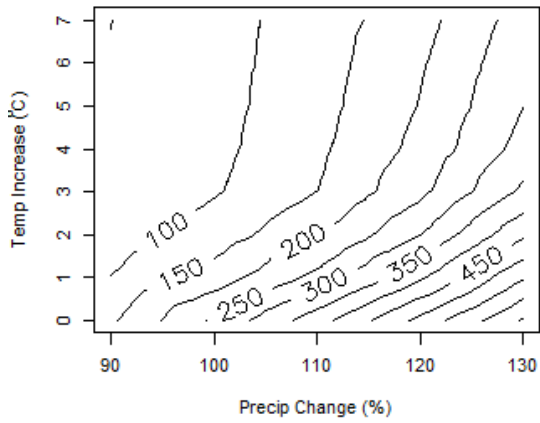
ASW 10 NTU - Jul

ASW 10 NTU - Aug
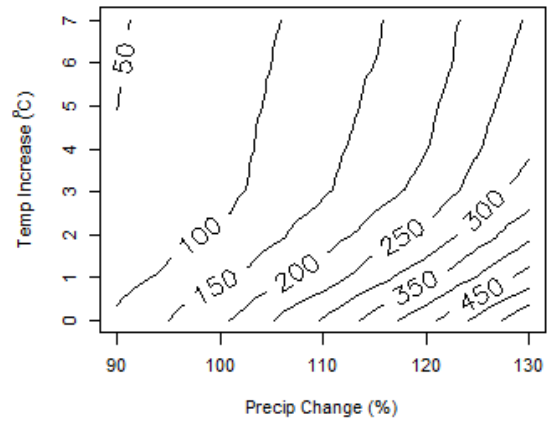
ASW 10 NTU - Sep
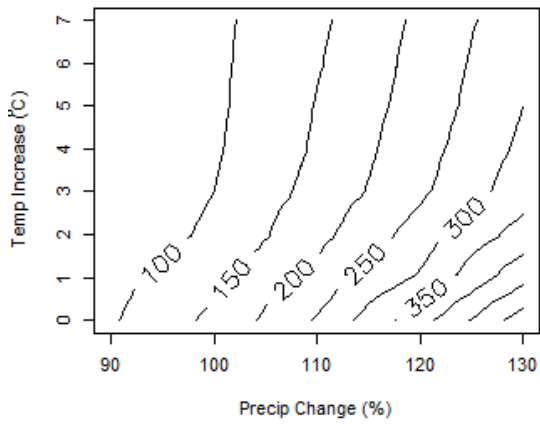
ASW 10 NTU - Oct
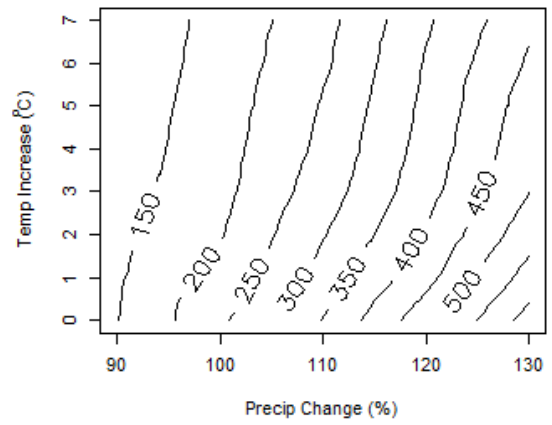
ASW 10 NTU - Nov
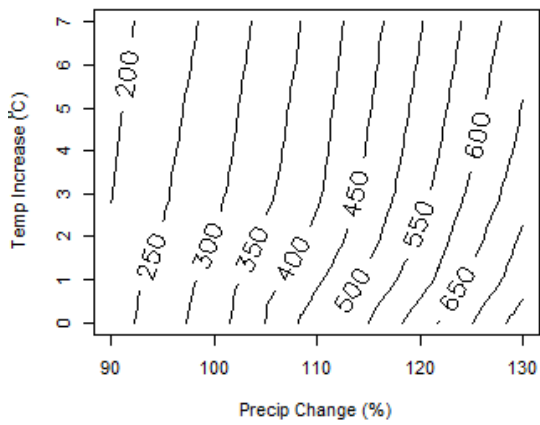
ASW 10 NTU - Dec
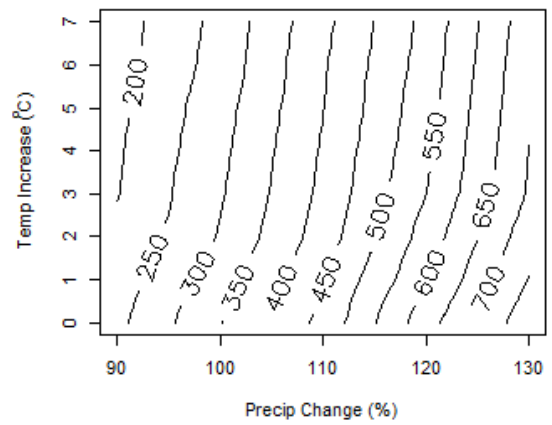
ASW 25 NTU - Jan
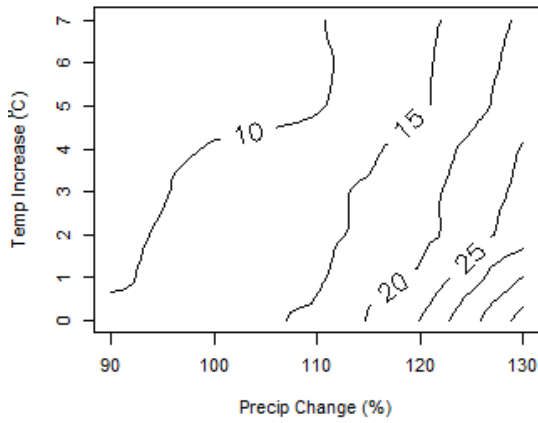
ASW 25 NTU - Feb
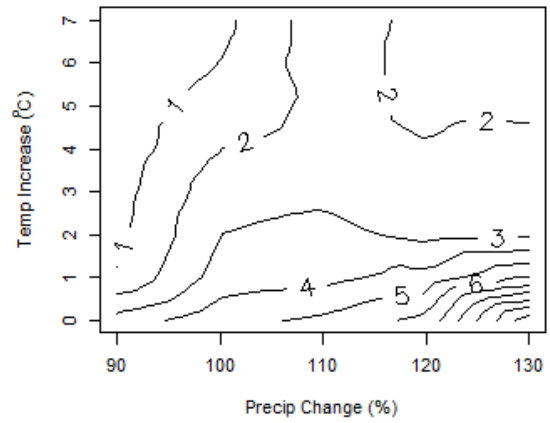
ASW 25 NTU - Mar
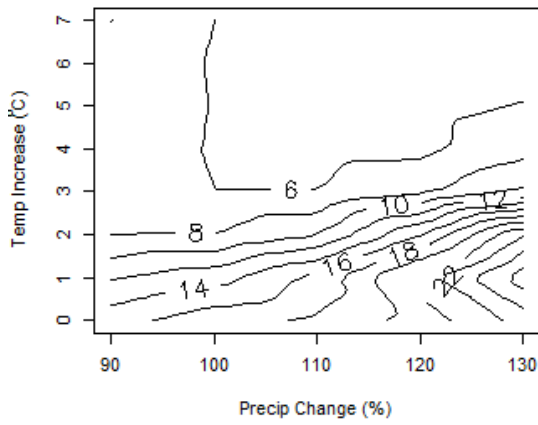
ASW 25 NTU - Apr
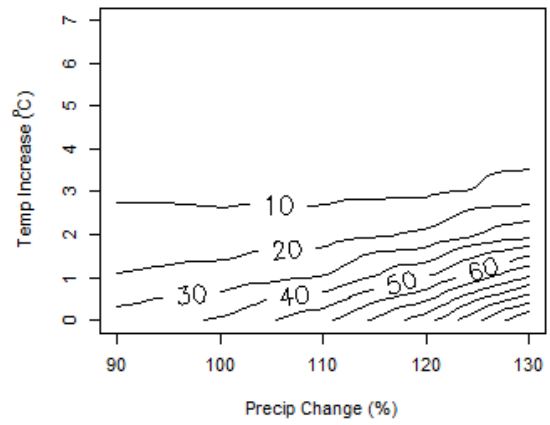
ASW 25 NTU - May
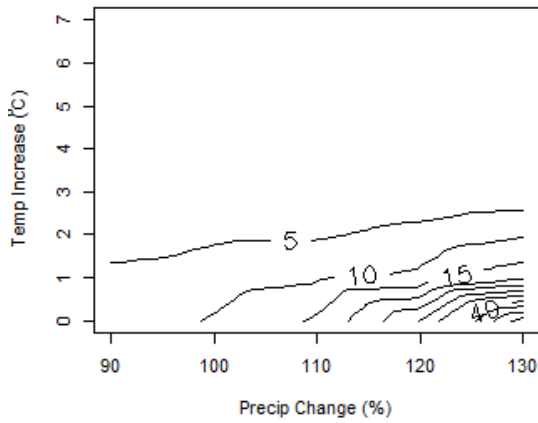
ASW 25 NTU - Jun
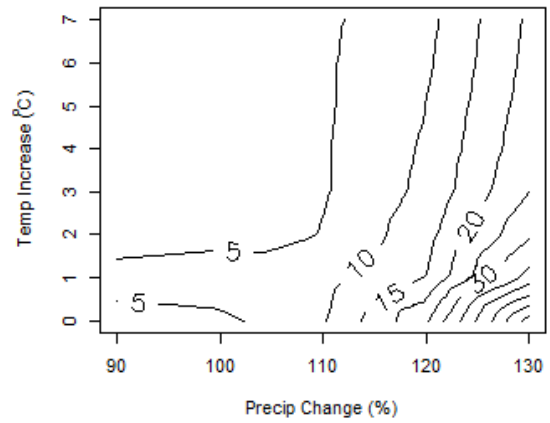
ASW 25 NTU - Jul
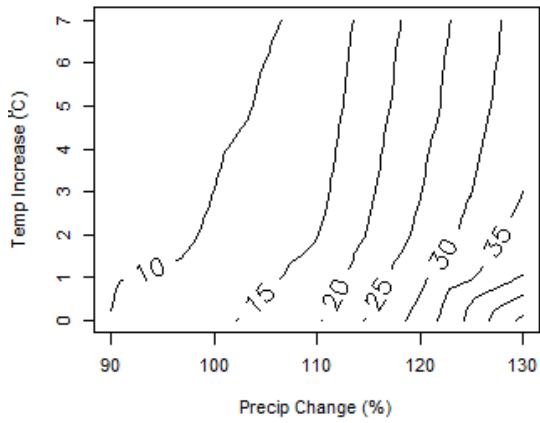
ASW 25 NTU - Aug
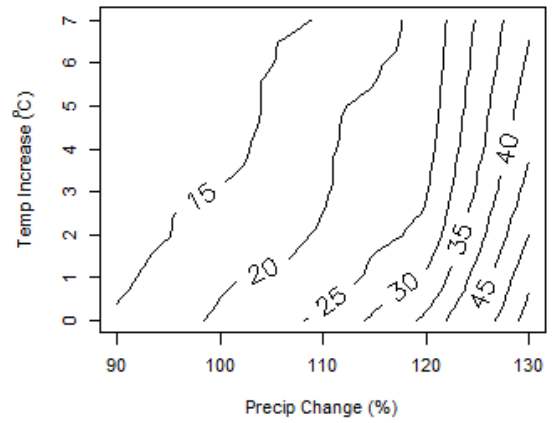
ASW 25 NTU - Sep
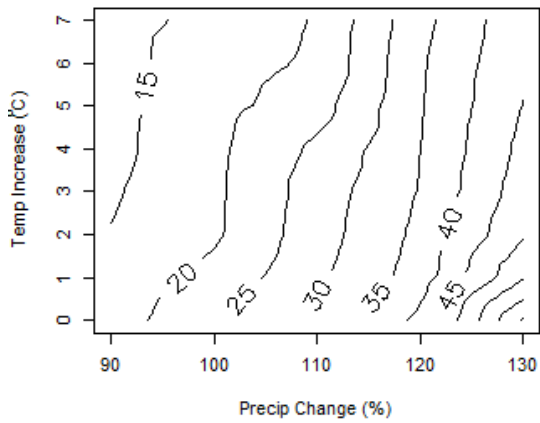
ASW 25 NTU - Oct
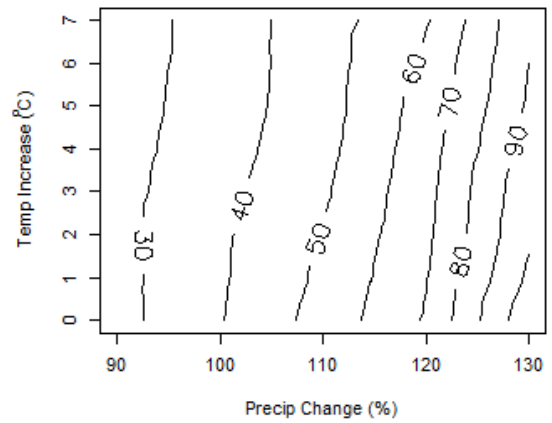
ASW 25 NTU - Nov
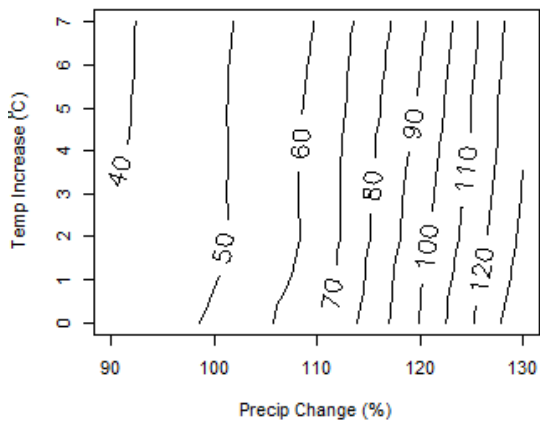
ASW 25 NTU - Dec
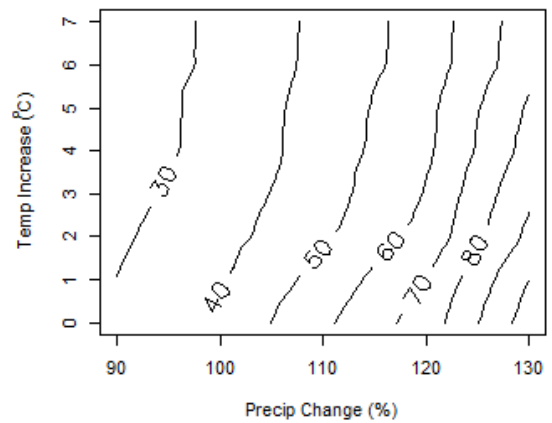
ASE 5 NTU - Jan
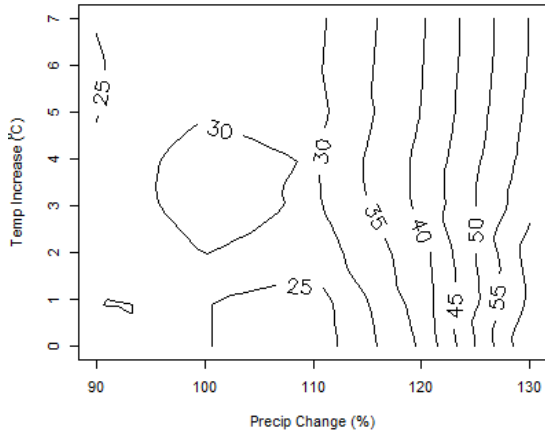
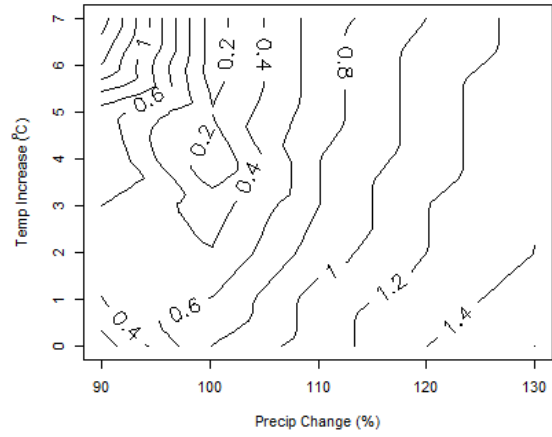**ASE 5 NTU - Feb**
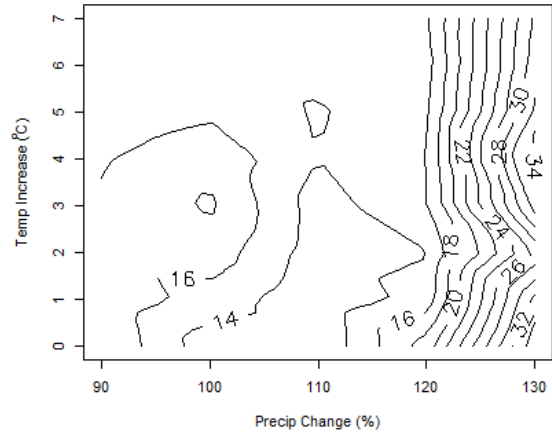
ASE 5 NTU - Mar
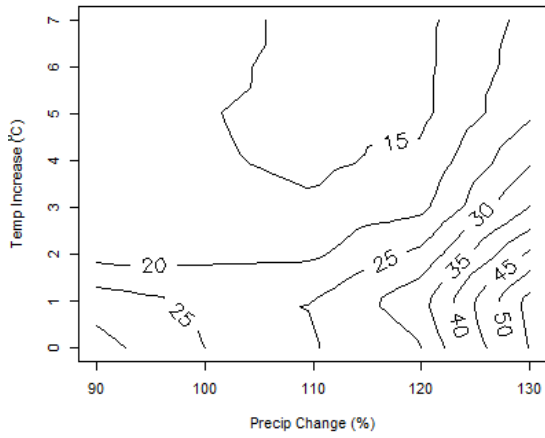
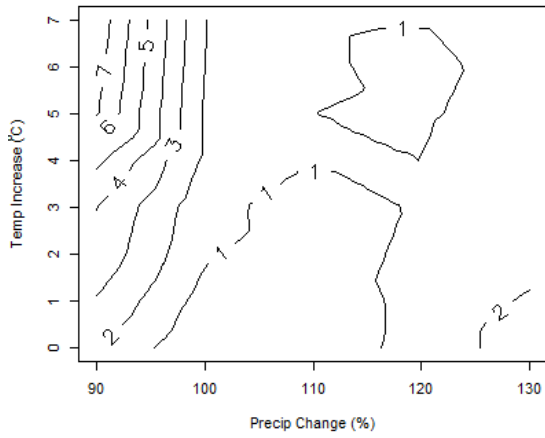**ASE 5 NTU - Apr**
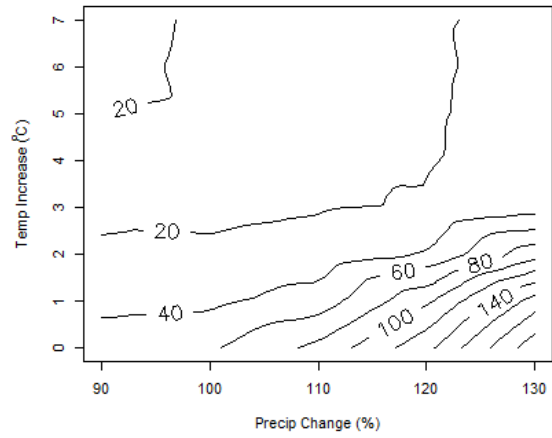
ASE 5 NTU - May
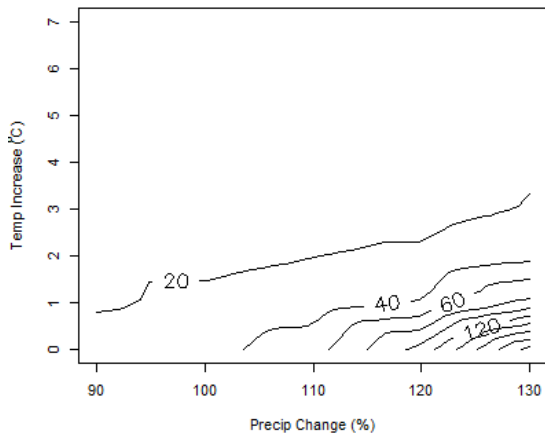
ASE 5 NTU - Jun
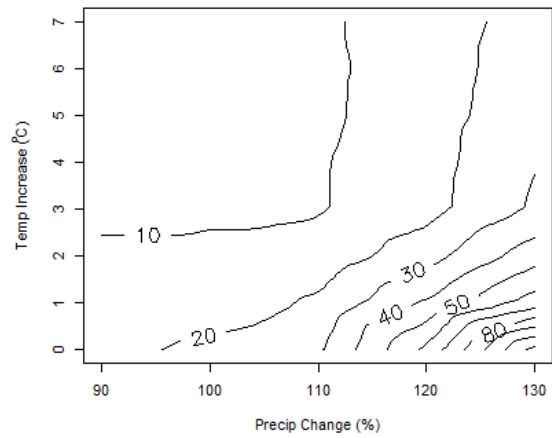
ASE 5 NTU - Jul
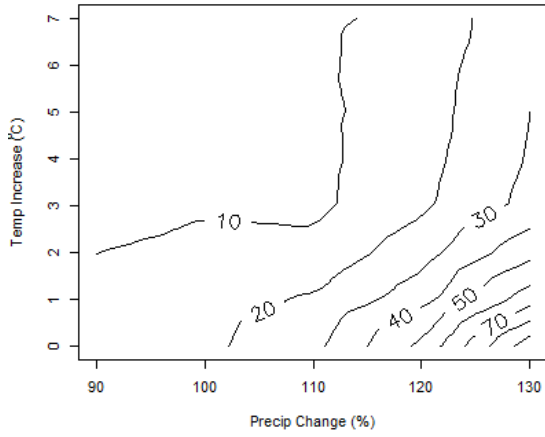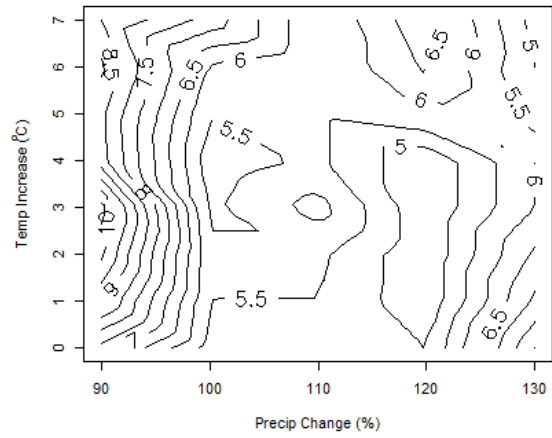
ASE 5 NTU - Aug
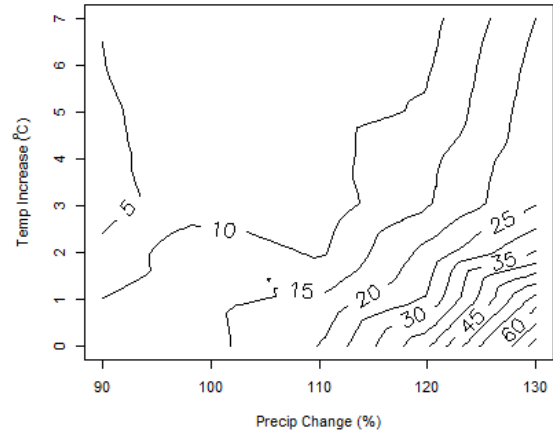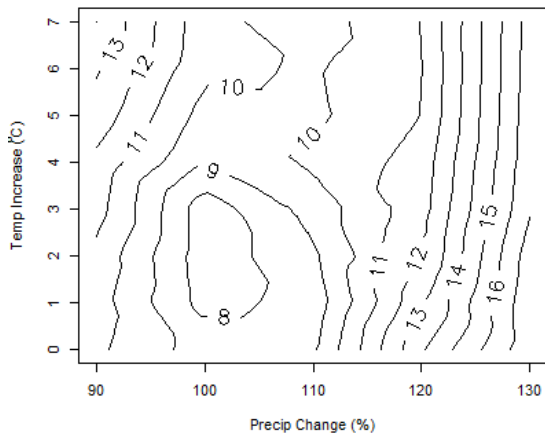
ASE 5 NTU - Sep
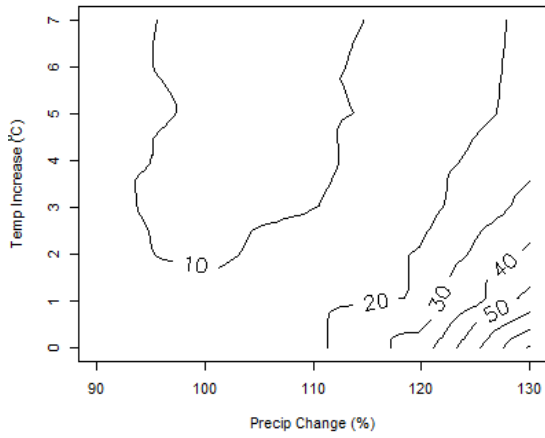
ASE 5 NTU - Oct
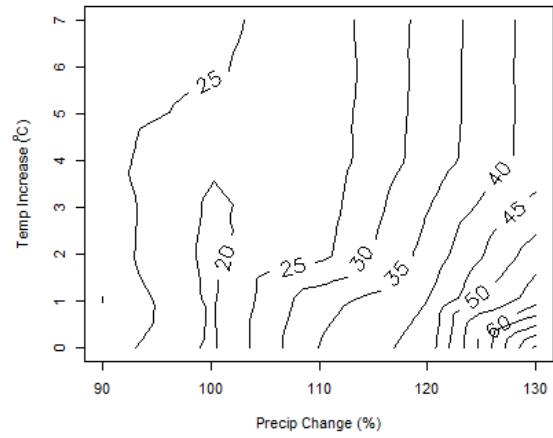
ASE 5 NTU - Nov
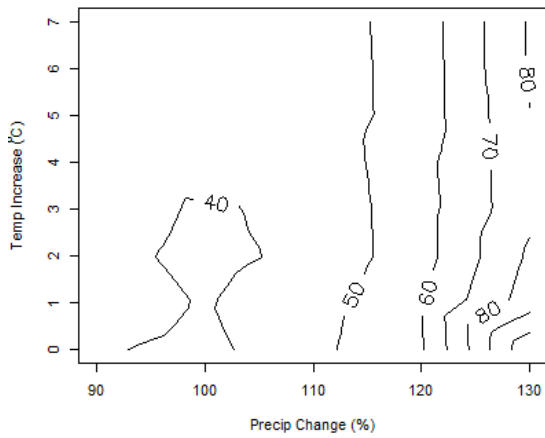
ASE 5 NTU - Dec
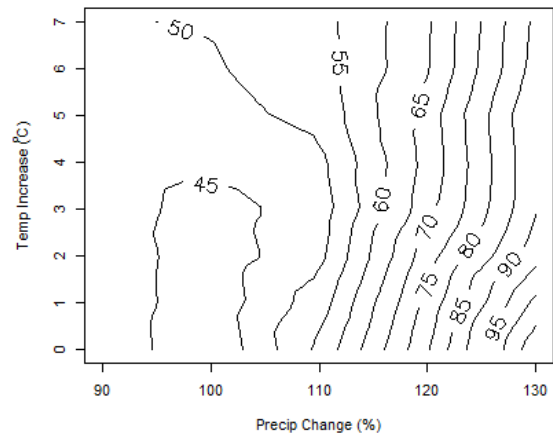
ASE 10 NTU - Jan
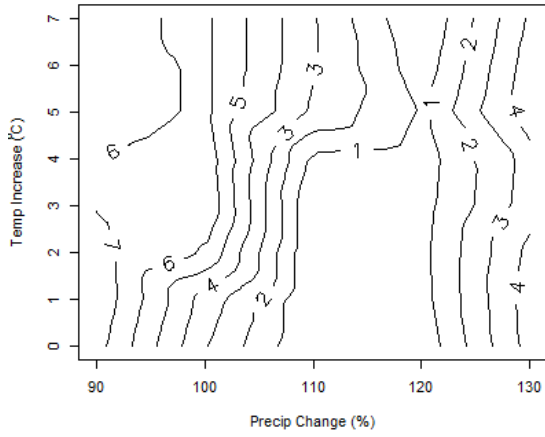
ASE 10 NTU - Feb
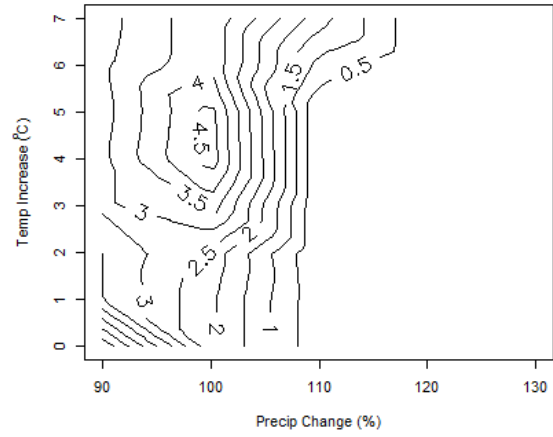
ASE 10 NTU - Mar
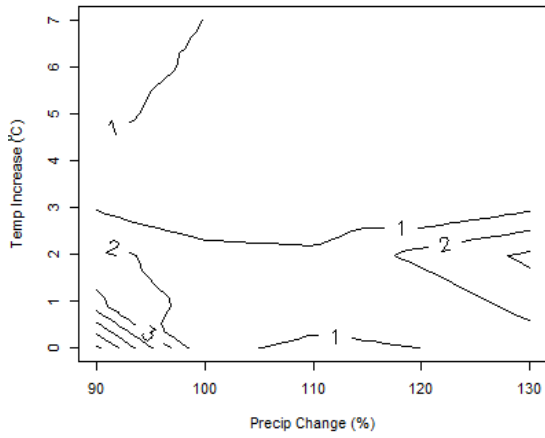
ASE 10 NTU - Apr
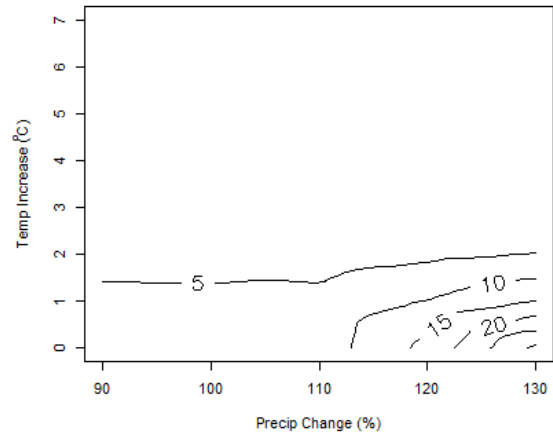
ASE 10 NTU - May
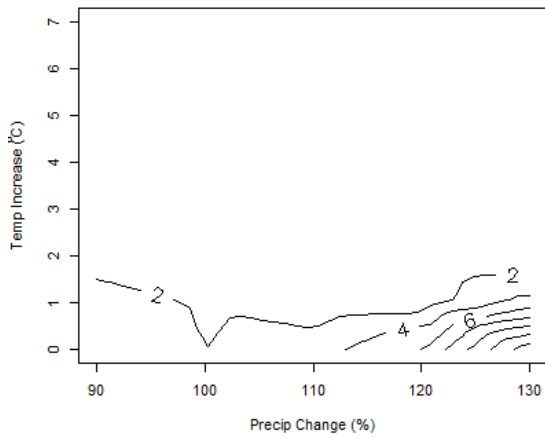
ASE 10 NTU - Jun
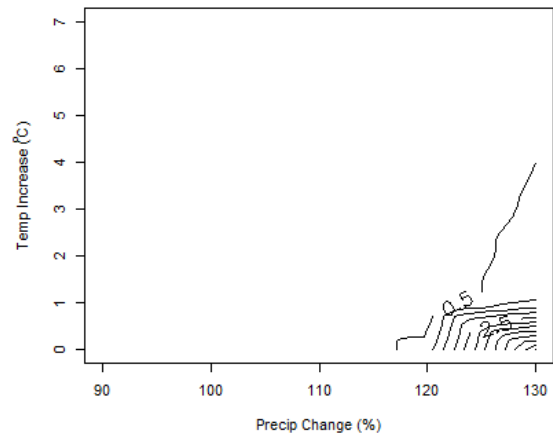
ASE 10 NTU - Jul
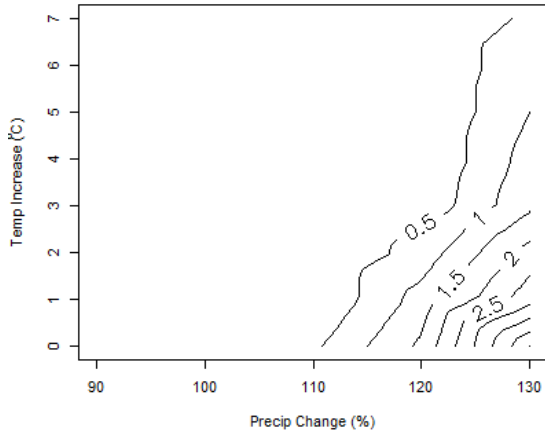
ASE 10 NTU - Aug

ASE 10 NTU - Sep

ASE 10 NTU - Oct

ASE 10 NTU - Nov

ASE 10 NTU - Dec